especially the posterior pole of the retina and fovea. (7) As a total sum of BOS24 for each attack in both eyes during a 6-month period, BOS24-6M presents disease activity for the patient during that period of time.

The BOS24 consists of a total 24 points summarized from 6 parameters of ocular inflammatory symptoms, including anterior chamber cells, vitreous opacity, peripheral fundus lesions, posterior pole lesions, subfoveal lesions, and optic disc lesions (Fig. 1; Table 1). Cells in the anterior chamber (maximum 4 points) are graded using the grading scale presented by the Standardization of Uveitis Nomenclature (SUN) Working Group [19], with a slight modification. Briefly, anterior chamber cells are detected and routinely scored using a semi-quantitative scoring system of 6 grades; 0 = no cells, 0.5+ = 1–5 cells per field, 1+ = 6–15 cells per field, 2+ = 16–25 cells per field, 3+ = 26–50 cells per field, and 4+ = 51 cells or more per field in the wide beam with a 1 × 1-mm narrow slit using slit-lamp microscopy. For convenience, cells in the anterior chamber scored as 0.5+ or 1+ in the SUN Working Group grading are noted as 1+ in the BOS24. Vitreous haze (maximum 4 points) is evaluated using the grading scale reported by Nussenblatt [20], with a slight modification. Briefly, vitreous haze is also graded using a semi-quantitative scoring system of 6 grades based on the clarity of the optic disc, retinal vessels, and nerve fiber layers; 4+ = optic disc is obscure, 3+ = optic disc can be seen but borders are quite blurry, 2+ = better visualization of retinal vessels, 1+ = better definition of optic nerve head and retinal vessels, trace = slight blurring of optic disc margin and reflex of the nerve fiber layer cannot be visualized, and 0 = no haze. For convenience, vitreous haze graded as trace and 1+ in the Nussenblatt grading is noted as 1+ in the BOS24. In the present study, chronic vitreous opacity was observed at every examination, but not scored with our scoring system.

For scoring retina inflammatory signs, the retinal field is divided into the posterior pole (areas inside of arcade vessels) and peripheral retina (areas outside of arcade vessels), with the latter further divided into 4 areas for each quadrant; temporal superior, temporal inferior, nasal superior, and nasal inferior. When scoring the peripheral retina, 2 points are added for each quadrant with new inflammatory signs, that is, any new retinal exudates or hemorrhages (maximum 8 points). Retinal edema is sometimes seen as chronic inflammation, thus it is not scored in the absence of other findings. When scoring the posterior pole of the retina, the percentage of the area of new inflammatory signs (hemorrhages, exudates) occupying areas of the posterior pole is first determined, with areas of retinal edema not included. The score is assigned 2 points if the percentage of the area of new inflammatory signs is less than 10 %, 3 points if the percentage is 10 % or more and less than 25 %, or 4 points if the percentage is 25 % or more.

As the fovea is considered to be especially important for affected patients, for any new hemorrhages or exudates observed in the fovea 2 points are added as the subfoveal lesion score. If there are new inflammatory signs for the optic disc (papillar edema usually accompanied by hemorrhages, exudates, retinal edema surrounding the optic disc), 2 points are added as the optic disc lesion score.

Determination of BOS24 validity

To determine the validity of our scoring system, 5 uveitis specialists (T.K., K.N., K.S, T.K., H.K.) examined the clinical records of 50 ocular attacks in 50 patients and estimated the severity of each. First, they determined the physician's impression score (1–10 points) of each of the 50 attacks based on the descriptions in the clinical records. The physician's impression score was determined based on simple impressions about the severity of the ocular attack in the same way as a visual analog scale (VAS), ranging from 1 to 10 points. They next determined the BOS24 scores independently, based on the descriptions of the clinical records. The scores were collected and the concordance rate among the 5 doctors was determined by calculating the coefficient of variance and maximum error rate using the following equations:

$$\text{coefficient of variance (CV)} = \text{standard deviation/average}$$

$$\text{maximum error rate (MER)} = \text{maximum error}^{*}\text{ (ME) / average}$$

*denotes maximum score among 5 doctors − minimum score among 5 doctors.

The variance and concordance of the scores between the 2 scoring methods were statistically examined using Student's paired *t*-test. In addition, the direct relationship between the doctor's impression score and BOS24 was examined with Spearman's rank-correlation coefficient.

BOS24 scoring before and after infliximab therapy

Patients in the present study had ocular BD, were referred to the uveitis clinics of 10 referral-based university hospitals in Japan and initially received infliximab therapy between January 2001 and December 2011. They were diagnosed with BD on the basis of criteria established by the Behçet's Disease Research Committee of Japan [20]. Briefly, those criteria for the complete type, include the presence of 4 major lesion types (oral aphthae, genital ulceration, uveitis, skin lesions), and for the incomplete type, 3 of those major lesions or uveitis, or 1 major lesion plus 2 minor lesions (arthritis, vascular lesion, central nervous system involvement, epididymitis and digestive organ lesions).

An open-label trial of infliximab was held in Japan from 2000 to 2005 for patients with refractory uveoretinitis due to BD who, despite the use of systemic anti-inflammatory/immunosuppressive drugs such as colchicine, cyclosporine, and/or systemic corticosteroid, continued to have ocular attacks, or were intolerant to such treatment. Infliximab was later approved in 2007 for patients with refractory uveoretinitis due to BD who, despite the use of systemic anti-inflammatory/immunosuppressive drugs, continued to have ocular attacks. In the present study, 190 patients who had received infliximab therapy for ocular BD were initially enrolled. However, 40 were excluded because they had no ocular attacks during the observation period (6 months before initiation of infliximab) or the scores of their ocular attacks from 6 months before the initiation of infliximab could not be determined because they had not undergone an examination at the time of the ocular attacks. Finally, a total of 150 patients (118 men, 32 women; age at initiation of infliximab 38.5 ± 12.1 years old) were enrolled to examine changes in BOS24. All patients in this study received infliximab therapy, as they continued to have ocular attacks, despite the use of systemic anti-inflammatory/immunosuppressive drugs or were intolerant of such treatment.

Data collection and statistical analysis

Clinical records were reviewed for gender, age of onset of uveitis, type of BD (complete or incomplete), visual acuity at the last remission each year from the onset of ocular disease, and medications received before and after initiation of infliximab therapy. In addition, the numbers of ocular attacks per eye during the 6 months before initiation of infliximab, the numbers of ocular attacks per eye every 6 months during the 3 years after initiation of infliximab therapy, and BOS24 for each ocular attack were examined by uveitis specialists by referring to the clinical records of each of the participating hospitals.

For this study, an ocular attack was defined as acute aggravation of intraocular inflammation with subjective symptoms of uveitis (conjunctival ciliary injection, floaters, blurred vision, etc.), and objective signs observed by slit-lamp microscopy and funduscopy [9]. To determine consensus among the uveitis specialists participating in this study, anterior chamber cells detected with slit-lamp microscopy were routinely scored using a semi-quantitative scoring system with 6 grades (0, 0.5+, 1+, 2+, 3+, 4+), as recommended by the SUN Working Group [19]. Vitreous opacity was also routinely scored using a semi-quantitative scoring system with 6 grades (0, 0.5+, 1+, 2+, 3+, 4+), as recommended by Nussenblatt et al. [20]. For the BOS24, cells in the anterior chamber (maximum 4 points) were graded using the scales presented by the SUN Working Group [19] and vitreous opacity (maximum 4 points) following Nussenblatt [20], both with slight modifications, as described above (Table 1). We considered that an increase in cells in the anterior chamber by grade 1+ or more indicated an ocular attack. Signs indicative of recent inflammation (obvious increase in vitreous opacity, retinal exudates, hemorrhages, vasculitis, edema) shown by funduscopy were also considered an ocular attack. Simultaneous bilateral attacks (attacks in both eyes) were considered to be 2 attacks, 1 attack in each eye, and BOS24 was separately determined for each eye.

The numbers of ocular inflammatory attacks during the 6-month periods before and after initiation of infliximab (pre 6, post 0–6, post 7–12, post 13–18, post 19–24, post 25–30, post 31–36 months) were determined for each patient. Moreover, the summation of BOS24 in a 6-month period, BOS24-6M, was calculated by adding up the BOS24 for every attack in the target 6-month period as a means of showing inflammatory activity during a given period of time. Best-corrected visual acuity was assessed using Landolt ring charts. Decimal best-corrected visual acuity was converted to a logarithm of the minimum angle of resolution prior to statistical analysis. Data collection forms were filled out by treating physicians at each participating center, and sent to a central data collection office (University of Tokyo Hospital) for collation and analysis.

Statistical analyses were conducted using Student's paired *t*-test, Fisher's exact probability test, Spearman's rank-correlation coefficient test, Wilcoxon signed-ranks test, or Mann–Whitney U test with SPSS for Windows version 14.0 (SPSS Inc., Chicago IL, USA). Values are shown as the mean ± SD and a level of $p < 0.05$ was accepted as statistically significant. This retrospective study was approved by the ethical committees of the University of Tokyo Hospital and collaborating hospitals.

Results

Validity of BOS24

To determine the validity of BOS24, 5 uveitis specialists examined 50 clinical records of ocular inflammatory attacks in patients with BD and noted their BOS24 and physician's impression score, as described in the Patients and methods Section. The average score for the 50 ocular attacks was 6.2 ± 3.3 with BOS24 and 4.2 ± 1.6 with doctor's impression scoring (Table 2), while the standard deviation was 0.65 ± 0.56 for BOS24 and 0.85 ± 0.42 for physician's impression scoring. The coefficient of variance among the 5 doctors was 11.1 ± 10.1 % for BOS24 and 19.9 ± 9.7 % for physician's impression score: significantly lower for BOS24 ($p < 0.0001$, Student's paired *t*-

Table 2 Variation of doctor's impression score and BOS24 among 5 uveitis specialists

	Doctor's impression score	BOS24	*p* value
Average score of 50 ocular attacks (points)	4.17 ± 1.63	6.18 ± 3.31	
Standard deviation of 50 ocular attacks (points)	0.85 ± 0.42	0.65 ± 0.56	
Coefficient of variance among 5 doctors (%)	19.9 ± 9.7	11.1 ± 10.1	<0.0001[a]
Maximum error (points)	2.06 ± 1.08	1.38 ± 1.21	0.0016[a]
Maximum error rate among 5 doctors (%)	48.3 ± 24.9	24.1 ± 22.8	<0.0001[a]
Perfect concordance cases of evaluation among 5 doctors (%)	5/50 (10)	16/50 (32)	0.0128[b]

[a] Student's paired *t*-test

[b] Fisher's exact probability test

test). Moreover, the maximum error among the 5 doctors was 1.38 ± 1.21 for BOS24 and 2.06 ± 1.08 for physician's impression score ($p = 0.0016$, Student's paired *t*-test), while the maximum error rate among them was 24.1 ± 22.8 % for BOS24 and 48.3 ± 24.9 % for physician's impression score ($p = 0.0016$, Student's paired *t*-test). Five (20 %) cases showed perfect concordance regarding physician's impression score and 16 regarding BOS24 among the 5 doctors ($p = 0.0128$, Fisher's exact probability test).

To clarify the relationship between the BOS24 and the physician's impression score, the averages for the 5 doctors were directly plotted and the correlations were examined using Spearman's rank-correlation coefficient test (Fig. 2).

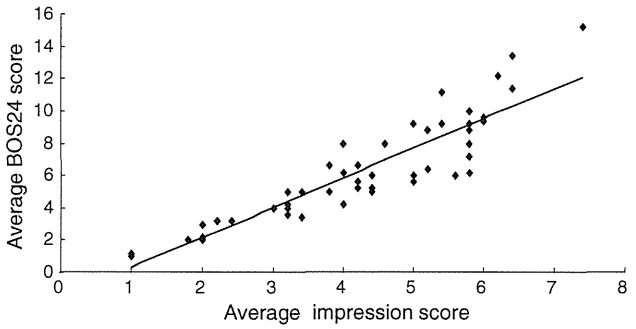

Fig. 2 Relationship between physician's impression score and BOS24. The average values for physician's impression score and BOS24 among 5 doctors for judgment of the same ocular attack were directly plotted, and the correlation was examined using Spearman's rank-correlation coefficient test. A strong relationship between physician's impression score and BOS24 was seen (the linear approximate equation used was as follows: $y = 1.8404x - 1.4948$, $R_s^2 = 0.926$; ρ value = 0.926, $p < 0.0001$, Spearman's rank-correlation coefficient test)

A strong relationship between the scoring systems was shown (ρ value = 0.926, $p < 0.0001$, Spearman's rank-correlation coefficient test), indicating that BOS24 was highly correlated with the physician's impression score and had a much lower variance.

Patient profiles

Baseline characteristics and pertinent medical histories for the 150 patients in this study are summarized in Table 3. Men comprised 79 % ($n = 118$). Age at the initiation of infliximab therapy was 38.5 ± 12.1 years old and 53 % ($n = 80$) of the patients were 20–39 years old. Most patients had a uveoretinitis duration of less than 10 years. The average number of ocular attacks in the 6-month period before starting infliximab was 3.2 ± 2.0 and all

Table 3 Baseline characteristics and relevant medical history of 150 patients

Characteristic	Value
Sex, no. (%)	
Male	118 (79)
Female	32 (21)
Age, years, no. (%)	
<20	7 (5)
20–39	80 (53)
40–59	53 (35)
≥60	10 (7)
Mean (SD)	38.5 (12.1)
Uveoretinitis duration, years, no. (%)	
<5	78 (52)
5–10	41 (27)
10–15	21 (14)
≥15	10 (7)
Mean (SD)	6.1 (5.3)
No. of ocular attacks in 6-month period before starting infliximab, no. (%)	
1–2	69 (16)
3–4	49 (21)
≥5	32 (33)
Mean (SD)	3.2 (2.0)
Cyclosporine use before starting infliximab, no. (%)	
Yes	63 (42)
No	87 (58)
Colchicine use before starting infliximab, no. (%)	
Yes	84 (56)
No	66 (44)
Oral corticosteroid use before starting infliximab, no. (%)	
Yes	55 (37)
No	95 (63)

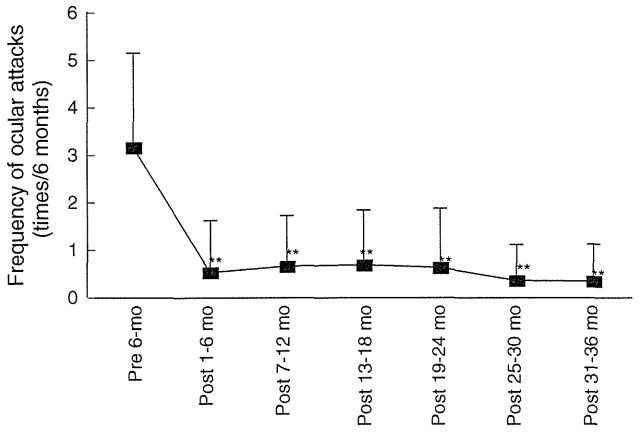

Fig. 3 Frequency of ocular attacks before and after initiation of infliximab. The numbers of ocular attacks in individual patients during each 6-month period before and after initiation of infliximab therapy were examined. Acute uveitis episodes during the 6-month period before treatment numbered 3.17 ± 2.00 (baseline), while those occurring from months 1–6, 7–12, 13–18, 19–24, 25–30, and 31–36 numbered 0.53 ± 1.10, 0.66 ± 1.07, 0.69 ± 1.15, 0.63 ± 1.25, 0.36 ± 0.75, and 0.35 ± 0.78, respectively. Statistical analysis was performed using Wilcoxon's signed-ranks test. $^{**}p < 0.0001$ as compared with baseline

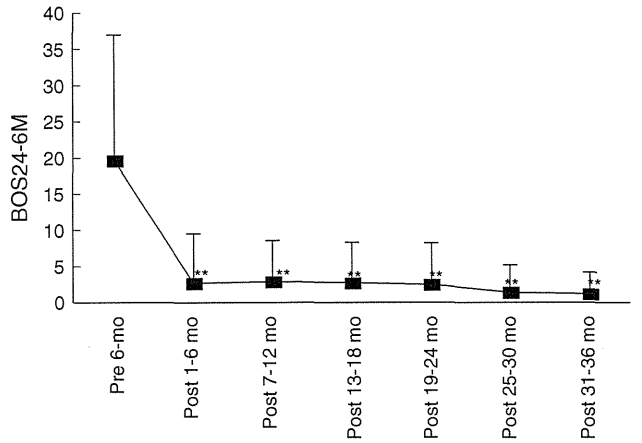

Fig. 4 Changes in BOS24-6M before and after initiation of infliximab. BOS24 in individual patients during the 6-month periods (BOS24-6M) before and after initiation of infliximab therapy were examined. The BOS24-6M value was 19.7 ± 17.4 during the 6-month period before treatment (baseline), while those in months 1–6, 7–12, 13–18, 19–24, 25–30, and 31–36 were 2.7 ± 6.9, 2.9 ± 5.7, 2.7 ± 5.6, 2.5 ± 5.8, 1.4 ± 3.8, and 1.2 ± 2.9, respectively. Statistical analysis was performed using Wilcoxon's signed-ranks test. $^{**}p < 0.0001$ as compared with baseline

patients had at least 1 attack during that period. Prior to starting infliximab, 42 % of the patients were using cyclosporine, 55 % colchicine, and 37 % oral corticosteroid, many of whom immediately discontinued cyclosporine and colchicine with infliximab therapy initiation, while others tapered to lower maintenance doses.

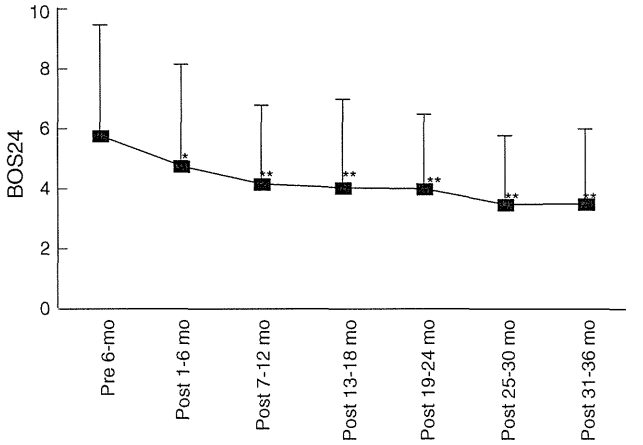

Fig. 5 Changes in BOS24 for individual ocular attacks before and after initiation of infliximab. The average BOS24 values for individual ocular attacks in each 6-month period before and after initiation of infliximab therapy were examined. The average BOS24 for an individual ocular attack during the 6-month period before initiation of infliximab (baseline) was 5.8 ± 3.7, while that for months 1–6 after treatment was 4.8 ± 3.4 ($p < 0.05$, Wilcoxon's signed rank test). Thereafter, the scores gradually decreased in months 7–12, 13–18, 19–24, 25–30, and 31–36 to 4.2 ± 2.6, 4.0 ± 3.0, 4.0 ± 2.5, 3.5 ± 2.3, and 3.5 ± 2.5, respectively ($^{*}p < 0.05$, $^{**}p < 0.0001$ as compared with baseline, Wilcoxon's signed-ranks test)

Frequency of ocular attacks and BOS24 before and after infliximab

As shown in Fig. 3, the number of ocular attacks in each patient decreased significantly from 3.2 ± 2.0 during the 6 months before starting infliximab (baseline) to 0.5 ± 1.1, 0.7 ± 1.1, 0.7 ± 1.2, 0.6 ± 1.3, 0.4 ± 0.8, and 0.4 ± 0.8 at 1–6, 7–12, 13–18, 19–24, 25–30, and 31–36 months, respectively, after starting therapy ($p < 0.001$ vs baseline for all 6 periods, Wilcoxon's signed rank test). In addition, as shown in Fig. 4, the BOS24-6M value also decreased significantly from 19.7 ± 17.4 at baseline to 2.7 ± 6.9, 2.9 ± 5.7, 2.7 ± 5.6, 2.5 ± 5.8, 1.4 ± 3.8, and 1.2 ± 2.9, respectively, during each 6-month period after initiation of therapy ($p < 0.001$ vs baseline for all 6 periods, $^{*}p < 0.0001$, Wilcoxon's signed rank test). These results demonstrated that infliximab therapy strongly suppressed the activity of uveitis due to BD.

Changes in BOS24 before and after starting infliximab therapy

To clarify the changes in ocular attacks before and after initiation of infliximab therapy, changes in BOS24 for each attack were examined (Fig. 5). The average BOS24 for individual ocular attacks was significantly decreased from 5.8 ± 3.7 at baseline to 4.8 ± 3.4 during the first 6 months

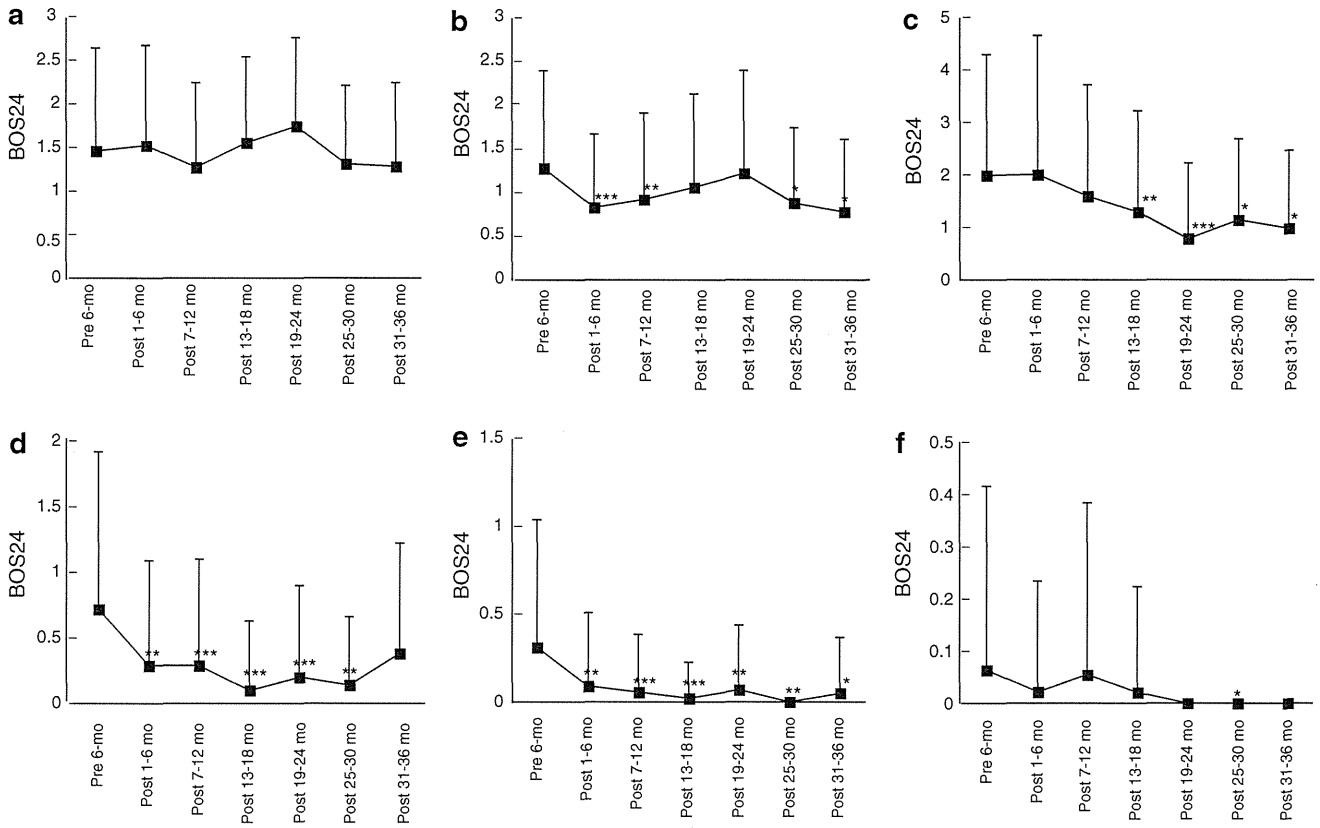

Fig. 6 Changes in BOS24 parameters for individual ocular attacks before and after initiation of infliximab. The average score for each of the 6 parameters of the BOS24 for individual ocular attacks during each 6-month period before (baseline) and after initiation of infliximab therapy were separately examined. **a** Anterior chamber cells, **b** vitreous opacity, **c** peripheral fundus lesions, **d** posterior pole lesions, **e** subfoveal lesions, and **f** optic disc lesions. Statistical analysis was performed using the Mann–Whitney U test. $^{*}p < 0.05$, $^{**}p < 0.01$, $^{***}p < 0.001$, as compared with baseline

after starting infliximab ($p < 0.05$, Wilcoxon's signed rank test) and then continued to decrease gradually in each 6-month period thereafter (4.2 ± 2.6, 4.0 ± 3.0, 4.0 ± 2.5, 3.5 ± 2.3, 3.5 ± 2.5, respectively; $p < 0.001$ vs baseline for all 5 periods, Wilcoxon's signed rank test). These results suggested that the severity of each ocular attack was suppressed after initiation of infliximab.

In addition, to examine changes in the characteristics of the ocular attacks with the initiation of infliximab therapy, the average scores for each of the 6 parameters of BOS24 for individual ocular attacks in each 6-month period were also investigated (Fig. 6). While the scores for anterior chamber cells and disc were not changed, those for vitreous opacity, peripheral retina, posterior pole of the retina, and fovea were significantly decreased in most of the periods after initiation of infliximab therapy (Fig. 6), with score reductions in the posterior pole of the retina and fovea especially prominent. These results suggested that infliximab therapy changes the characteristics of ocular attacks, especially those accompanying lesions in the posterior pole of the retina and fovea.

Discussion

The characteristics of uveitis due to BD are (1) recurrent acute ocular inflammation (so-called ocular inflammatory attacks), (2) acute iridocyclitis, so strong that it is sometimes accompanied by hypopyon, and (3) uveoretinitis causing retinal exudates and/or hemorrhages that are sometimes accompanied by occlusion of retinal vessels. These ocular inflammatory lesions are usually transient and disappear spontaneously, even if no treatment is administrated. Thus, evaluation of ocular inflammatory activity is difficult, because its severity can vary greatly between appointments.

Evaluation of ocular inflammatory activity is mainly performed based on frequency of the ocular inflammatory attacks [5–7, 10, 11] or type of inflammatory attacks, such as anterior uveitis only or anterior and posterior uveitis [11, 12], presence or absence of severe ocular inflammation signs (hypopyon, involvement of inflammation of retina, macula, or optic disc) [11], or physicians' impression of severity (i.e. mild, moderate, severe) [13, 14]. The BDCAF

is a popular clinical instrument used to assess the systemic activity of BD [13, 14]. The scoring is based on the history of new clinical features presented over the 4 weeks prior to assessment. Determination of ocular disease activity with the BDCAF is dependent on patients' answers to questions regarding whether symptoms (red eye, blurred vision, eye pain) were present during the preceding 4 weeks. However, the definitions of the points in the scale are imprecise, especially regarding ocular diseases. We, therefore, decided to establish a more definite scoring system to evaluate ocular disease activity in BD patients, termed BOS24.

The BOS24 consists of a total 24 points that sum up 6 parameters of ocular inflammatory signs dependent on the severity of clinical inflammatory signs in the eyes, with focus on the characteristics of ocular attacks in BD patients. Since this scoring system consists of only objective findings and no subjective rating such as patient impression, it is preferable as a tool for scientific analysis. Furthermore, the BOS24 may be useful as a complement to the BDCAF when evaluating ocular status. We believe that the BOS24 is uniquely specialized for the characteristics of ocular BD and optimal for evaluation for related disease activity.

In the present study, we first assessed the reliability and validity of BOS24. Five uveitis specialists examined the clinical records of 50 BD patients in regard to ocular inflammatory attacks using the BOS24 and doctor's impression (1–10 points) scores. Using those findings, we determined the differences between BOS24 and physician's impression scoring among 5 doctors. The coefficient of variance was significantly lower for BOS24 ($p < 0.0001$, Student's paired t test, Table 3), while the maximum error rate among the doctors was also significantly lower for BOS24 ($p = 0.0016$, Student's paired t-test). Moreover, a strong relationship between physician's impression score and BOS24 score was shown by scattered plot analysis (ρ value $= 0.926, p < 0.0001$, Spearman's rank-correlation coefficient test, Fig. 2). Together, these results suggest that BOS24 is highly correlated with scores based on physician's impression, with a much lower variance among doctors as compared with physician's impression scoring.

In our comparison between BOS24 and clinical impression score for validation of our system, some observer bias was noted when the same patients were scored by the two systems, which might have been reduced by the use of a masked independent physician scoring method. On the other hand, fairness in the comparison of the two scoring systems may have also been reduced, because different doctors evaluated each of the scoring systems. Thus, it seems impossible to completely negate the bias due to the limitations of the study design.

Using our scoring system, we also examined changes in ocular disease activity before and after initiation of infliximab therapy. A total of 150 patients treated at 10 regional university hospitals in Japan for ocular BD with infliximab were enrolled to examine changes in BOS24 both before and after starting therapy. As expected, both the number of ocular attacks during each 6-month examination period, and total BOS24 in various 6-month periods (BOS24-6M) decreased dramatically after starting infliximab (Figs. 3, 4). In addition, the average BOS24 score for each ocular attack decreased after starting therapy (Fig. 5). These results suggest that infliximab has the potential to reduce not only the frequency of ocular attacks, but also ocular disease activities in BD. Furthermore, our results obtained with the BOS24 are the first to show that the severity of each ocular attack was also suppressed by infliximab administration.

When we analyzed the 6 parameters of the BOS24 for each ocular attack, scores for vitreous opacity, peripheral retina, posterior pole of the retina, and foveal lesions decreased significantly during most of the examined periods after beginning therapy, with score reduction in the posterior pole of the retina and fovea especially prominent (Fig. 6). These results indicate that infliximab has the potential to reduce the frequency of ocular attacks, especially in the posterior poles, including the fovea. This is very important because inflammation in the posterior poles including the fovea leads directly to permanent visual loss. Furthermore, these results confirm the report by Okada, who noted reductions in the severity of ocular attacks after initiation of infliximab therapy [8]. In 50 cases of BD examined in that study, 133 ocular inflammatory attacks were observed in the 6-month period before the initiation of infliximab, of which 96 (72 %) were moderate or severe. On the other hand, 22 attacks were observed in the 6-month period after initiation of infliximab, of which only 7 (32 %) were moderate or severe. The present study confirmed those results and also clarified the portions affected by the ocular attacks in detail. On the other hand, we were unable to determine the precise mechanism related to prevention of ocular attacks in those areas, though such information might be greatly beneficial for preventing loss of visual acuity in patients with refractory uveitis due to BD.

The BOS24 scoring system is simple to use, as it is based on new inflammatory signs in the eyes. Thus, we think that most ophthalmologists by observing and noting fresh inflammatory signs, such as cells in the anterior chamber, vitreous haze, retinal hemorrhages, exudates and vasculitis, can utilize this novel system. In addition, our goal was to make the BOS24 scoring system simple enough to use retrospectively with medical records. Nevertheless, there are some limitations to this system. For example, ocular attacks cannot be scored if the patient does not undergo an examination during an ocular attack.

Furthermore, it is difficult to score retinal lesions if ocular fundus lesions are invisible due to vitreous opacity, vitreous hemorrhages, or the presence of a cataract. Thus, previous scoring systems including the number of attacks and BCVA remain the most established methods of evaluation of ocular disease activities in patients with BD. However, counting the number of attacks based on patient complaints without a medical examination can also be inaccurate. For example, if the patient notes blurred vision in the absence of a true ocular inflammatory attack, the number of attacks may be miscounted. All scoring systems have limitations, including BOS24. In the present study, no scoring was possible for patients who did not visit a hospital during an ocular attack or in cases with invisible ocular fundus lesions, thus those were not included in the BOS24-6M total. Nevertheless, we consider that this novel system is useful and reliable, as it can be used by doctors to evaluate the severity of ocular attacks by assessing new inflammatory signs in the eyes. Moreover, we believe that BOS24-6M is an excellent method for evaluating ocular disease activities, as it considers not only the frequency of ocular inflammatory attacks, but also the severity of each. Further evaluations, minor changes to the system, and accumulation of evidence are necessary.

In conclusion, we developed a novel disease activity scoring system for determining ocular inflammation in patients with BD, termed BOS24. Our findings demonstrate that the results of the system were well correlated with physician's impression scores and had significantly higher reproducibility among doctors. Using BOS24, we found that infliximab therapy reduced not only the total scores for disease activity during specific 6-month periods (BOS24-6M), but also the severity of individual ocular attacks. The reduction of scores after initiation of therapy was particularly high in the posterior portion of the retina and fovea, demonstrating that infliximab has potential for preventing loss of visual acuity. Nevertheless, a prospective study may be necessary to clarify the effectiveness of infliximab on disease activity in patients with ocular BD. We believe that BOS24 is a promising tool for evaluating ocular BD activities.

Acknowledgments This study was supported in part by a Grant-in-Aid for Science Research for Behçet's disease from the Ministry of Health, Labor and Welfare of Japan (No. 087100000332).

Conflicts of interest T. Kaburaki, None; K. Namba, None; K. Sonoda, None; T. Kezuka, Lecture fees (Mitsubishi Tanabe Pharma); H. Keino, None; T. Fukuhara, None; K. Kamoi, None; K. Nakai, None; N. Mizuki, None; N. Ohguro, None; The Ocular Behçet Disease Research Group of Japan, None.

Appendix: Group information

The members of the Ocular Behçet's Disease Research Group of Japan are as follows:

Hokkaido University, Sapporo: Kenichi Namba M.D., Ph.D.*, Shigeaki Ohno M.D., Ph.D. and Nobuyoshi Kitaichi M.D., Ph.D.

Kyorin University, Tokyo: Hiroshi Keino M.D., Ph.D.*, Annabelle A. Okada M.D., Ph.D. and Takayo Watanabe M.D., Ph.D.

Kyushu University, Fukuoka: Takako Fukuhara M.D.*, Atsunobu Takeda M.D., Ph.D. and Tatsuro Ishibashi M.D., Ph.D.

Osaka Koseinenkin Hospital, Osaka: Nobuyuki Ohguro M.D., Ph.D.* and Kenji Yawata M.D.

Osaka University Graduate School of Medicine, Osaka: Kei Nakai M.D., Ph.D.* and Chiharu Iwahashi M.D., Ph.D.

Tokyo Medical and Dental University, Tokyo: Koju Kamoi M.D., Ph.D.*, Manabu Mochizuki M.D., Ph.D. and Sunao Sugita M.D., Ph.D.

Tokyo Medical University, Tokyo: Takeshi Kezuka M.D., Ph.D.* and Hiroshi Goto M.D., Ph.D.

University of Tokyo, Tokyo: Toshikatsu Kaburaki M.D., Ph.D.*, Mitsuko Takamoto M.D., Ph.D. and Hisae Nakahara M.D.

Yamaguchi University, Yamaguchi: Koh-hei Sonoda M.D., Ph.D.* and Yukiko Kondo MD, PhD.

Yokohama City University, Yokohama: Nobuhisa Mizuki M.D., Ph.D.*, Etsuko Shibuya M.D., Ph.D. and Ikuko Kimura M.D.

*The Writing Group for the Ocular Behcet's Disease Research Group of Japan.

References

1. Ohguro N, Sonoda KH, Takeuchi M, Matsumura M, Mochizuki M. The 2009 prospective multi-center epidemiologic survey of uveitis in Japan. Jpn J Ophthalmol. 2012;56:432–5.
2. Nakae K, Masaki F, Hashimoto F, Inaba G, Mochizuki M, Sakane T. Recent epidemiological features of Behçet's disease in Japan. In: Godeau P, Wechsler B, editors. Behçet's disease. Amsterdam: Excerpta Medica; 1993. p. 145–51.
3. Mochizuki M, Akduman L, Nussenblatt RB. Behçet disease. In: Pepose JS, Holland GN, Wilhelmus KR, editors. Ocular infection and immunity. St. Louis: Mosby; 1996. p. 663–75.
4. Evereklioglu C. Current concepts in the etiology and treatment of Behçet disease. Surv Ophthalmol. 2005;50:297–350.
5. Ohno S, Nakamura S, Hori S, Shimakawa M, Kawashima H, Mochizuki M, et al. Efficacy, safety, and pharmacokinetics of multiple administration of infliximab in Behçet's disease with refractory uveoretinitis. J Rheumatol. 2004;31:1362–8.
6. Sfikakis PP, Theodossiadis PG, Katsiari CG, Kaklamanis P, Markomichelakis NN. Effect of infliximab on sight-threatening panuveitis in Behçet's disease. Lancet. 2001;358:295–6.
7. Niccoli L, Nannini C, Benucci M, Chindamo D, Cassarà E, Salvarani C, et al. Long-term efficacy of infliximab in refractory posterior uveitis of Behçet's disease: a 24-month follow-up study. Rheumatology. 2007;46:1161–4.
8. Sfikakis PP, Iliopoulos A, Elezoglou A, Kittas C, Stratigos A. Psoriasis induced by anti-tumor necrosis factor therapy. Arthritis Rheum. 2005;52:2513–8.

9. Kawazoe Y, Sugita S, Yamada Y, Akino A, Miura K, Mochizuki M. Psoriasis triggered by infliximab in a patient with Behçet's disease. Jpn J Ophthalmol. 2013;57:95–7.
10. Yoshida A, Kawashima H, Motoyama Y, Shibui H, Kaburaki T, Shimizu K, et al. Comparison of patients with Behcet's disease in the 1980s and 1990s. Ophthalmology. 2004;111:810–5.
11. Okada AA, Goto H, Ohno S, Mochizuki M, Ocular Behçet's Disease Research Group of Japan. Multicenter study of infliximab for refractory uveoretinitis in Behçet disease. Arch Ophthalmol. 2012;130:592–8.
12. Kaburaki T, Araki F, Takamoto M, Okinaga K, Yoshida A, Numaga J, et al. Best-corrected visual acuity and frequency of ocular attacks during the initial 10 years in patients with Behçet's disease. Graefes Arch Clin Exp Ophthalmol. 2010;248:709–14.
13. Bhakta BB, Brennan P, James TE, Chamberlain MA, Noble BA, Silman AJ. Behçet's disease: evaluation of a new instrument to measure clinical activity. Rheumatology (Oxford). 1999;38: 728–33.
14. Lawton G, Bhakta BB, Chamberlain MA, Tennant A. The Behcet's disease activity index. Rheumatology (Oxford). 2004;43: 73–8.
15. Gaujoux-Viala C, Mouterde G, Baillet A, Claudepierre P, Fautrel B, Le Loët X, et al. Evaluating disease activity in rheumatoid arthritis: which composite index is best? A systematic literature analysis of studies comparing the psychometric properties of the DAS, DAS28, SDAI and CDAI. Joint Bone Spine. 2012;79: 149–55.
16. Prevoo ML, van 't Hof MA, Kuper HH, van Leeuwen MA, van de Putte LB, van Riel PL. Modified disease activity scores that include twenty-eight-joint counts. Development and validation in a prospective longitudinal study of patients with rheumatoid arthritis. Arthritis Rheum. 1995;38:44–8.
17. Smolen JS, Breedveld FC, Schiff MH, Kalden JR, Emery P, Eberl G, et al. A simplified disease activity index for rheumatoid arthritis for use in clinical practice. Rheumatology. 2003;42: 244–57.
18. Aletaha D, Nell VP, Stamm T, Uffmann M, Pflugbeil S, Machold K, et al. Acute phase reactants add little to composite disease activity indices for rheumatoid arthritis: validation of a clinical activity score. Arthritis Res Ther. 2005;7:R796–806.
19. Jabs DA, Nussenblatt RB, Rosenbaum JT. Standardization of Uveitis Nomenclature (SUN) Working Group. Standardization of uveitis nomenclature for reporting clinical data. Results of the First International Workshop. Am J Ophthalmol. 2005;140: 509–16.
20. Nussenblatt RB, Palestine AG, Chan CC, Roberge F. Standardization of vitreal inflammatory activity in intermediate and posterior uveitis. Ophthalmology. 1985;92:467–71.

Protection of Human Corneal Epithelial Cells From TNF-α–Induced Disruption of Barrier Function by Rebamipide

Kazuhiro Kimura,[1] Yukiko Morita,[1] Tomoko Orita,[1] Junpei Haruta,[2] Yasuhiro Takeji,[2] and Koh-Hei Sonoda[1]

[1]Department of Ophthalmology, Yamaguchi University Graduate School of Medicine, Ube, Yamaguchi, Japan
[2]Ako Research Institute, Otsuka Pharmaceutical Co., Ltd., Ako, Hyogo, Japan

Correspondence: Kazuhiro Kimura, Department of Ophthalmology, Yamaguchi University Graduate School of Medicine, 1-1-1 Minami-Kogushi, Ube, Yamaguchi 755-8505, Japan; k.kimura@yamaguchi-u.ac.jp.

Submitted: November 13, 2012
Accepted: March 1, 2013

Citation: Kimura K, Morita Y, Orita T, Haruta J, Takeji Y, Sonoda K-H. Protection of human corneal epithelial cells from TNF-α–induced disruption of barrier function by reamipide. *Invest Ophthamol Vis Sci.* 2013;54:2752–2760. DOI:10.1167/iovs.12-11294

Purpose. TNF-α disrupts the barrier function of cultured human corneal epithelial (HCE) cells. We investigated the effects of the cytoprotective drug rebamipide on this barrier disruption by TNF-α as well as on corneal epithelial damage in a rat model of dry eye.

Methods. The barrier function of HCE cells was evaluated by measurement of transepithelial electrical resistance. The distribution of tight-junction (ZO-1, occludin) and adherens-junction (E-cadherin, β-catenin) proteins, and the p65 subunit of nuclear factor-κB (NF-κB) was determined by immunofluorescence microscopy. Expression of junctional proteins as well as phosphorylation of the NF-κB inhibitor IκB-α and myosin light chain (MLC) were examined by immunoblot analysis. A rat model of dry eye was developed by surgical removal of exorbital lacrimal glands.

Results. Rebamipide inhibited the disruption of barrier function as well as the downregulation of ZO-1 expression, and the disappearance of ZO-1 from the interfaces of neighboring HCE cells induced by TNF-α. It also inhibited the phosphorylation and downregulation of IκB-α, the translocation of p65 to the nucleus, the formation of actin stress fibers, and the phosphorylation of MLC induced by TNF-α in HCE cells. Treatment with rebamipide eyedrops promoted the healing of corneal epithelial defects as well as attenuated the loss of ZO-1 from the surface of corneal epithelial cells in rats.

Conclusions. Rebamipide protects corneal epithelial cells from the TNF-α–induced disruption of barrier function by maintaining the distribution and expression of ZO-1 as well as the organization of the actin cytoskeleton. Rebamipide is, thus, a potential drug for preventing or ameliorating the loss of corneal epithelial barrier function associated with ocular inflammation.

Keywords: cytokine, corneal epithelium, wound healing, barrier

The corneal epithelium serves as a barrier to protect the eye from external agents such as microbes and chemicals as well as to maintain corneal transparency.[1–3] The formation of tight junctions (TJs) between adjacent epithelial cells at the apical plasma membrane[4,5] gives rise to both a physical and functional barrier.[6] Adherens junctions (AJs) between epithelial cells play an important role in the formation of TJs.[7] The protein components of TJs include zonula occludens (ZO-1, ZO-2, and ZO-3), occludin, claudin, and junctional adhesion molecules (JAMs),[8,9] whereas AJs are composed of cadherins and catenins (α-catenin, β-catenin, p120 catenin).[10,11] Both AJ and TJ components are tightly linked to the actin cytoskeleton.[12,13] ZO-1, occludin, claudin, E-cadherin, and β-catenin have been detected in the corneal epithelium[14–16] and are thought to determine its barrier function.[17–22]

The inflammatory response to a variety of insults such as injury and infection includes the production of various cytokines and chemokines. TNF-α, a proinflammatory cytokine,[23] contributes to ocular inflammation such as that associated with infection,[24] injury,[25] and dry eye.[26] Ocular inflammation associated with ocular surface diseases has been shown to affect corneal structure and function.[27,28] The concentration of TNF-α in tear fluid has been found to be markedly increased in patients with dry eye.[29] Moreover, the amount of TNF-α at the ocular surface is increased in a mouse model of dry eye.[26,30,31]

Rebamipide was selected from among more than 500 amino acid analogs of 2(1*H*)-quinolinone tested for the ability to prevent the development and to promote the healing of gastric ulcers by stimulating the production of prostaglandins by the gastric mucosa.[32] It also exhibits anti-inflammatory activity in the esophagus and stomach as a result of its inhibition of the production of cytokines and chemokines by several cell types.[33,34] Corneal damage including structural irregularities and haze induced by ultraviolet B radiation has also been found to be attenuated by rebamipide in mice.[35]

We have previously shown that TNF-α disrupts the barrier function of cultured human corneal epithelial (HCE) cells.[21] In the present study, we examined the effect of rebamipide on the loss of transepithelial electrical resistance (TER) induced by TNF-α in these cells. We also investigated the effects of rebamipide on the expression and distribution of TJ and AJ proteins, on the nuclear factor (NF)-κB signaling pathway, and on the actin cytoskeleton in corneal epithelial cells exposed to TNF-α. Finally, we examined the effect of administration of rebamipide eyedrops on corneal epithelial damage in a rat model of dry eye induced by removal of lacrimal glands.

METHODS

Materials

Dulbecco's modified Eagle's medium nutrient mixture F-12 (DMEM/F-12), PBS, fetal bovine serum, trypsin-EDTA, and gentamicin were all obtained from Invitrogen-Gibco (Carlsbad, CA). Bovine serum albumin (BSA), recombinant bovine insulin, cholera toxin, recombinant human epidermal growth factor, a mouse monoclonal antibody to myosin light chain (MLC), and a protease inhibitor cocktail were all from Sigma-Aldrich (St. Louis, MO). Six- or 24-well transwell plates as well as 24-well culture plates were obtained from Corning (Corning, NY). Rabbit polyclonal antibodies to the p65 subunit of NF-κB and mouse monoclonal antibodies to IκB-α or to phosphorylated IκB-α were obtained from Santa Cruz Biotechnology (Santa Cruz, CA). Rabbit polyclonal antibodies to phosphorylated MLC were from Cell Signaling (Danvers, MA), whereas those to ZO-1 or to occludin were from Zymed (San Francisco, CA). Mouse monoclonal antibodies to E-cadherin or to β-catenin were obtained from BD Biosciences (Carlsbad, CA). Cyto59, horseradish peroxidase–conjugated, or AlexaFluor 488–labeled goat antibodies to mouse or rabbit immunoglobulin G, and rhodamine-phalloidin were from Invitrogen-Gibco. ECL Plus reagents were obtained from GE Healthcare (Little Chalfont, UK). 2-(4-Chlorobenzamido)-3-[2(1*H*)-quinolinon-4-yl]propionic acid (rebamipide) was obtained from Tokyo Chemical Industry (Tokyo, Japan). Rebamipide ophthalmic suspension (2%) and vehicle (the same solution without rebamipide) were formulated at Otsuka Pharmaceutical Co., Ltd. (Ako, Hyogo, Japan).

Cells and Cell Culture

Simian virus 40–immortalized HCE cells[36] were obtained from RIKEN Biosource Center (Tokyo, Japan). They were passaged in supplemented hormonal epithelial medium (SHEM), which comprises DMEM/F-12 supplemented with 15% heat-inactivated fetal bovine serum, bovine insulin (5 μg/mL), cholera toxin (0.1 μg/mL), human epidermal growth factor (10 ng/mL), and gentamicin (40 μg/mL). For experiments, HCE cells were plated at a density of 1×10^5 or 3×10^5 cells per well in 24- or 6-well transwell plates (filter pore size of 0.4 μm), respectively, or at 1×10^5 cells per well in 24-well culture plates. They were then cultured for 4 days in SHEM and for 24 hours in unsupplemented DMEM/F-12 before incubation first for 12 hours with or without rebamipide and then for the indicated times in the additional absence or presence of TNF-α (10 ng/mL) in unsupplemented DMEM/F-12. Rebamipide was dissolved in unsupplemented DMEM/F-12 at a concentration of 2 mM (stock solution) for HCE cell experiments.

Measurement of TER

The TER of HCE cells cultured in 24-well transwell plates was measured with the use of an Epithelial Volt-ohm meter (EVOM; World Precision Instruments, Sarasota, FL).[21,22] TER (ohms × centimeter squared) was calculated by multiplying the measured resistance by the area of the transwell filter. The background resistance due to the filter alone (~130 ohms × cm^2) was measured before cell plating and was subtracted from the experimental values.

Immunofluorescence Analysis

HCE cells were cultured in 24-well culture plates. For ZO-1, occludin, E-cadherin, and β-catenin staining, the cells were fixed with 100% methanol for 20 minutes at room temperature. For staining of the p65 subunit of NF-κB, the cells were fixed with 4% paraformaldehyde in PBS, washed with PBS, and permeabilized with 100% methanol for 5 minutes at −20°C. All cells were then washed with PBS and incubated at room temperature for 1 hour with 1% BSA in PBS and then for 1 hour with antibodies to ZO-1, to occludin, to E-cadherin, to β-catenin, or to p65, each at a 1:100 dilution in PBS containing 1% BSA. After washing with PBS, the cells were incubated at room temperature for 1 hour with AlexaFluor 488–labeled secondary antibodies at a 1:1000 dilution in PBS containing 1% BSA, and then for 10 minutes with Cyto59 for staining of nuclei. For staining of the actin cytoskeleton, cells fixed and permeabilized as for staining of p65 were incubated for 1 hour at room temperature with rhodamine-phalloidin at a 1:100 dilution in PBS containing 1% BSA. All cells were then examined with a laser confocal microscope (LSM5; Zeiss, Oberkochen, Germany). The intensity of ZO-1 immunofluorescence was measured with the use of the National Institutes of Health ImageJ software (version 1.46r; Bethesda, MD).

Immunoblot Analysis

HCE cells cultured in 6-well transwell plates were lysed in 300 μL of a solution containing 50 mM Tris-HCl (pH 7.5), 150 mM NaCl, 1 mM EDTA, 5 mM NaF, 1% Nonidet P-40, 0.5% sodium deoxycholate, 0.1% SDS, 1 mM Na_3VO_4, and 1% protease inhibitor cocktail. The lysates were centrifuged at 15,000*g* for 10 minutes at 4°C, and the resulting supernatants were subjected to SDS-PAGE on a 10% gel. The separated proteins were transferred to a nitrocellulose membrane, which was then incubated at room temperature first for 1 hour with blocking buffer (20 mM Tris-HCl [pH 7.4], 5% dried skim milk, 0.1% Tween 20) and then for 2 hours with primary antibodies, each at a 1:1000 dilution in blocking buffer. The membrane was washed with washing buffer (20 mM Tris-HCl [pH 7.4], 0.1% Tween 20), incubated for 1 hour at room temperature with horseradish peroxidase–conjugated goat secondary antibodies (1:1000 dilution in washing buffer), washed again, incubated with ECL Plus detection reagents for 5 minutes, and then exposed to film.

Rat Model of Dry Eye and Evaluation of Corneal Epithelial Damage

Male 4-week-old Sprague-Dawley rats were obtained from SLC Japan (Shizuoka, Japan). All animal procedures were performed in accordance with the ARVO Statement for the Use of Animals in Ophthalmic and Vision Research and were approved by the animal experimentation committee of Yamaguchi University Graduate School of Medicine. A rat dry eye model was prepared.[37] In brief, rats at 5 weeks of age were anesthetized by intraperitoneal injection of pentobarbital sodium for bilateral removal of the exorbital lacrimal glands. Dry eye was evaluated 5 weeks after surgery by staining of the cornea with 1 μL of 1% fluorescein in saline. Excess fluorescein was washed out from the eye with saline, and corneal staining was photographed with the use of a confocal laser-scanning ophthalmoscope (F-10; NIDEK, Aichi, Japan). The rats ($n = 8$ per group) were then treated four times daily for 4 weeks in each eye with 5 μL of 2% rebamipide ophthalmic suspension or corresponding vehicle. The extent of corneal epithelial damage was evaluated by fluorescein staining at 4, 7, 14, 21, and 28 days after the onset of treatment. For evaluation of staining, photographs of the cornea were divided transversely into three sections and each section was scored from 0 to 3 (0, no staining; 1, scattered staining [punctate or dispersed]; 2, moderate staining; 3, pronounced staining) by an observer not aware of whether the eye received rebamipide or vehicle.

Investigative Ophthalmology & Visual Science

The scores for the three sections were summed to give the total score for the cornea (maximum score of 9).

After the final evaluation of corneal epithelial damage, rats were killed with a lethal dose of pentobarbital sodium, the eyes were enucleated, and each cornea was isolated, and cut into four tissue blocks. The tissue was fixed with acetone for 15 minutes at room temperature, washed with PBS, permeabilized with 0.1% Triton X-100 in PBS for 10 minutes, and then incubated with PBS containing 1% BSA for 1 hour to block nonspecific binding of antibodies. The tissue was then incubated overnight at 4°C with antibodies to ZO-1 (1:100 dilution), washed with PBS, incubated for 1 hour at room temperature with Alexa Fluor 488–conjugated secondary antibodies (1:200 dilution), washed with PBS, and stained with 4′,6-diamidino-2-phenylindole. The tissue blocks were then examined with a laser confocal microscope (LSM5; Zeiss) as described previously for immunofluorescence analysis of HCE cells. The ZO-1 signal was binarized and the defective area of ZO-1 staining was measured with ImageJ software (version 1.46r; National Institutes of Health).

Statistical Analysis

Quantitative data are presented as means ± SEM. Differences between two groups were analyzed with Student's nonparametric *t*-test, and those among multiple groups were evaluated with ANOVA followed by Dunnett's multiple-comparison test. A P value of less than 0.05 was considered statistically significant.

Results

We have previously shown that TNF-α downregulates the barrier function of cultured HCE cells.[21] To examine the effect of rebamipide on the TNF-α–induced disruption of barrier function in these cells, we measured TER. A confluent monolayer of HCE cells was cultured in serum-free medium for 24 hours and then exposed to various concentrations of rebamipide (0–0.3 mM) for 12 hours before incubation in the additional presence of TNF-α for 24 hours. Whereas TNF-α reduced the TER of HCE cells, this effect was inhibited by rebamipide in a concentration-dependent manner, with the action of rebamipide being significant at 0.1 and 0.3 mM (Fig. 1).

We next examined by immunofluorescence analysis the effects of rebamipide on the distribution of TJ (ZO-1 and occludin) and AJ (E-cadherin and β-catenin) proteins in HCE cells exposed to TNF-α. We previously showed that TNF-α induced the disappearance of ZO-1 from the cell border,[21] and this effect was significantly inhibited by rebamipide at 0.3 mM (Fig. 2). TNF-α did not affect the localization of occludin, E-cadherin, or β-catenin at the borders of adjacent cells, and rebamipide also had no effect on the localization of these proteins in the presence of TNF-α (Fig. 2).

We previously showed that TNF-α downregulated the amount of ZO-1 in HCE cells.[21] Immunoblot analysis revealed that rebamipide significantly inhibited this effect of TNF-α (Fig. 3). TNF-α did not affect the abundance of occludin, E-cadherin, or β-catenin, and rebamipide also had no effect on the expression of these proteins in the presence of TNF-α (Fig. 3).

NF-κB activation is required for the TNF-α–induced disruption of barrier function in HCE cells[21]; therefore, we next examined the effect of rebamipide on NF-κB activation induced by TNF-α in these cells. Incubation of the cells with rebamipide for 12 hours before exposure to TNF-α markedly inhibited both the phosphorylation and degradation of the endogenous NF-κB inhibitor IκB-α (Fig. 4A) as well as the translocation of the p65 subunit of NF-κB to the nucleus (Fig. 4B) induced by TNF-α.

We next examined the effect of rebamipide on the reorganization of the actin cytoskeleton induced by TNF-α. TNF-α induced the formation of actin stress fibers in HCE cells, and this effect was inhibited by rebamipide (Fig. 5A). TNF-α also induced the phosphorylation of MLC in HCE cells in a manner sensitive to inhibition by rebamipide (Fig. 5B).

Finally, we examined the effect of eyedrops containing rebamipide on corneal epithelial damage in a rat model of dry eye induced by bilateral removal of the exorbital lacrimal glands. Eyedrops containing rebamipide (2%) were adminis-

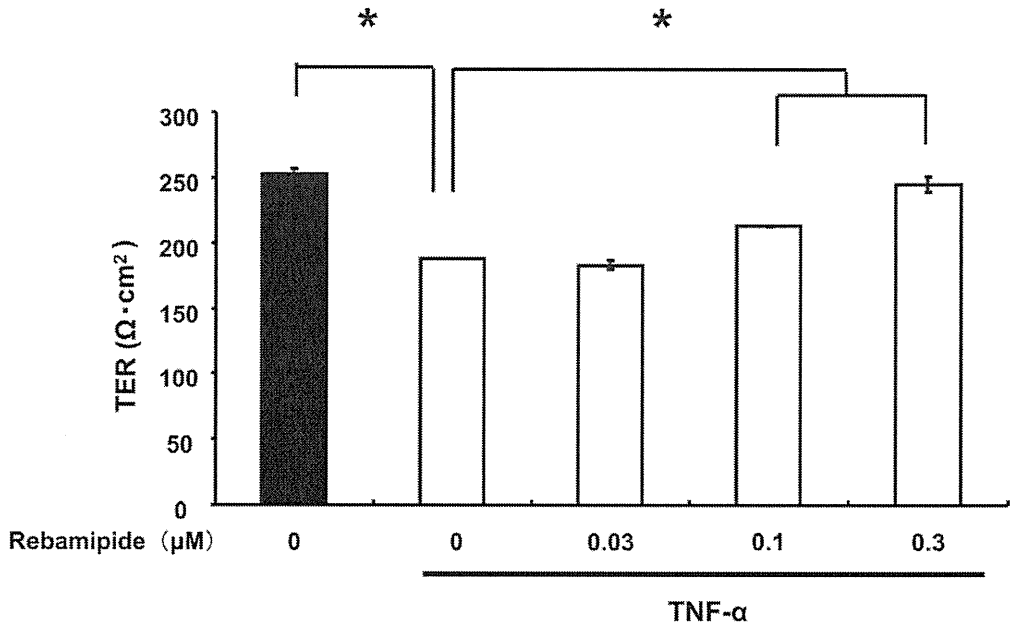

FIGURE 1. Effect of rebamipide on the TNF-α–induced loss of barrier function in HCE cells. Cells were cultured with the indicated concentrations of rebamipide for 12 hours and then in the additional absence (*closed bar*) or presence (*open bars*) of TNF-α for 24 hours, after which TER of the cell monolayer was measured. Data are means ± SEM from four independent experiments. *$P < 0.05$ (ANOVA followed by Dunnett's test).

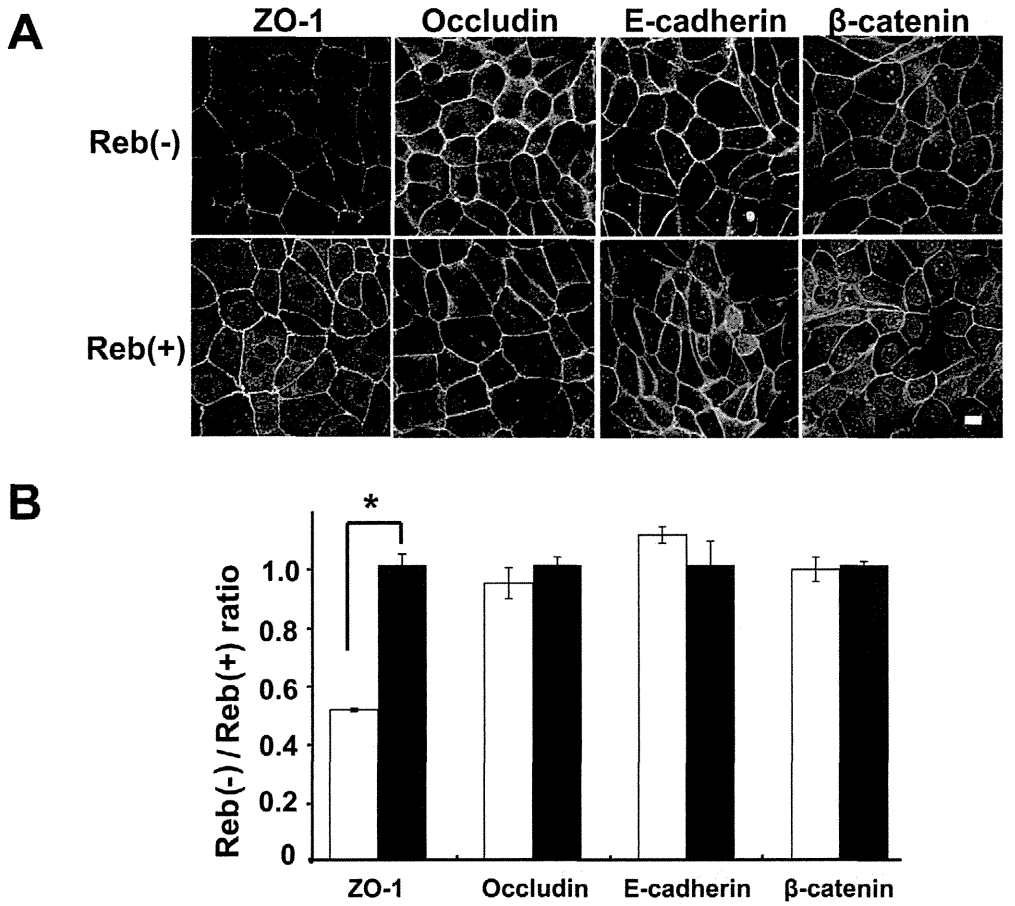

FIGURE 2. Effect of rebamipide on the distribution of junctional proteins in HCE cells exposed to TNF-α. (**A**) Cells were incubated in the absence or presence of rebamipide (Reb; 0.3 mM) for 12 hours and then in the additional presence of TNF-α for 24 hours, after which they were fixed and subjected to immunofluorescence analysis with antibodies to ZO-1, to occludin, to E-cadherin, or to β-catenin. *Scale bar*: 10 μm. (**B**) Quantitation of immunofluorescence staining for cells treated as in (**A**). The mean fluorescence intensity at cell–cell borders at four points chosen at random was determined by image analysis. Data are means ± SEM from three independent experiments. $^*P < 0.05$ (Student's unpaired *t*-test).

tered at 6 hour intervals for 28 days. Fluorescein staining revealed that rebamipide induced significant resurfacing of the corneal epithelial defects in this model compared with eyes treated with vehicle (Fig. 6). We also examined the distribution of ZO-1 in the corneal epithelium at the end of the treatment period. Immunofluorescence analysis revealed that, whereas ZO-1 was localized at the interfaces of adjacent corneal epithelial cells in the healthy eye, removal of the lacrimal glands resulted in a loss of ZO-1 immunoreactivity from the borders of superficial epithelial cells in defective areas and that this effect was greatly attenuated by rebamipide treatment (Fig. 7).

DISCUSSION

We have shown that rebamipide inhibited the TNF-α–induced decrease in TER of HCE cells in a concentration-dependent manner. This effect of rebamipide was associated with inhibition of the TNF-α–induced disappearance of ZO-1 from the borders of adjacent HCE cells as well as of the TNF-α–induced downregulation of ZO-1 expression. Rebamipide did not affect the distribution or abundance of occludin, E-cadherin, or β-catenin in HCE cells exposed to TNF-α. The activation of NF-κB signaling, formation of actin stress fibers, and phosphorylation of MLC induced by TNF-α were also attenuated by rebamipide. These results, thus, suggest that rebamipide inhibits the TNF-α–induced disruption of barrier function in cultured corneal epithelial cells by maintaining the expression and distribution of ZO-1. Furthermore, rebamipide ameliorated the corneal epithelial damage as well as inhibited the loss of ZO-1 from the borders of corneal epithelial cells induced by removal of lacrimal glands in a rat model of dry eye. Rebamipide, thus, also appears to protect the corneal epithelium from disruption of barrier function in vivo.

Rebamipide inhibits the disruption of barrier function in gastric and intestinal epithelial cells as well as in other epithelial cell types.[38,39] We now show that rebamipide protects against barrier disruption associated with the downregulation of ZO-1 expression and the loss of ZO-1 from cell–cell borders induced by TNF-α in HCE cells, and that it exerts similar effects in a rat model of dry eye. These results suggest that rebamipide may regulate barrier function by modulating the expression and localization of the TJ protein ZO-1 in corneal epithelial cells.

TJ and AJ proteins are associated with perijunctional actin filaments, which modulate barrier function.[40,41] The contraction and rearrangement of the actin cytoskeleton, thus, contribute to barrier disruption.[8,42,43] The phosphorylation of MLC induces the reorganization of perijunctional actin and disrupts TJs.[44] We have now shown that rebamipide inhibited TNF-α–induced MLC phosphorylation and rearrangement of the actin cytoskeleton in HCE cells, suggesting that rebamipide modulates the linkage between junctional complexes and the

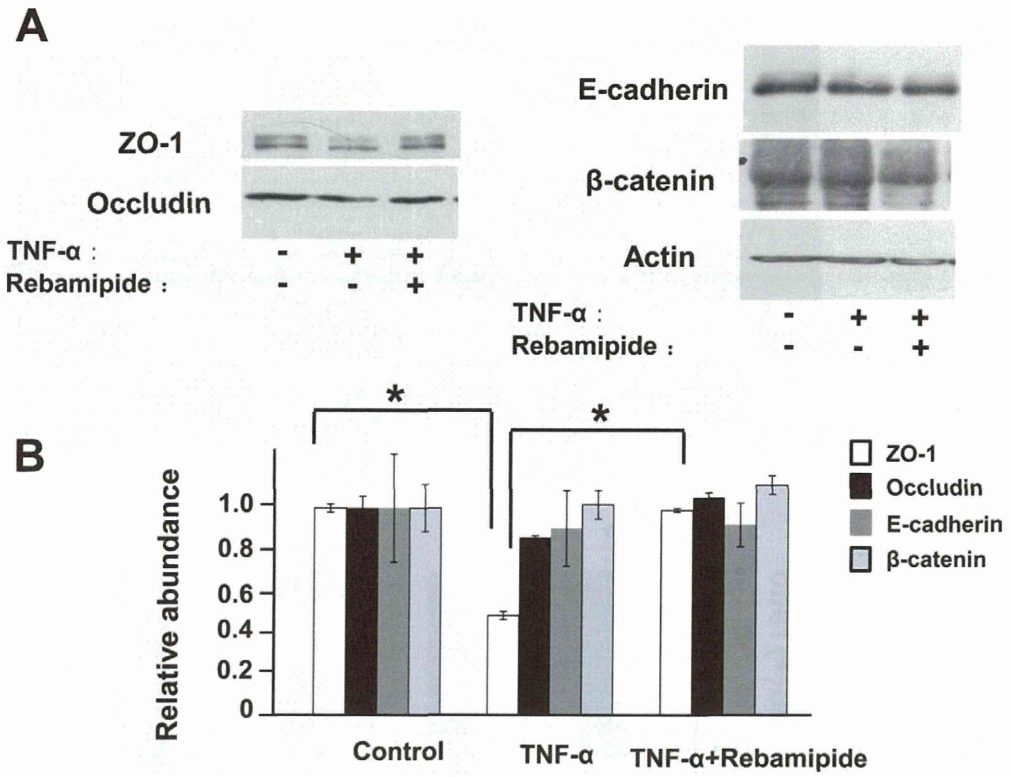

FIGURE 3. Effect of rebamipide on the expression of junctional proteins in HCE cells exposed to TNF-α. (**A**) Cells were incubated in the absence or presence of rebamipide (0.3 mM) for 12 hours and then in the additional absence or presence of TNF-α for 24 hours, after which cell lysates were prepared and subjected to immunoblot analysis with antibodies to ZO-1, to occludin, to E-cadherin, to β-catenin, or to β-actin (loading control). (**B**) Immunoblots similar to those in (**A**) were subjected to densitometric analysis for determination of the abundance of each junctional protein normalized by that of β-actin. Data are expressed relative to the corresponding value for control cells and are means ± SEM from three independent experiments. *$P < 0.05$ (ANOVA followed by Dunnett's test).

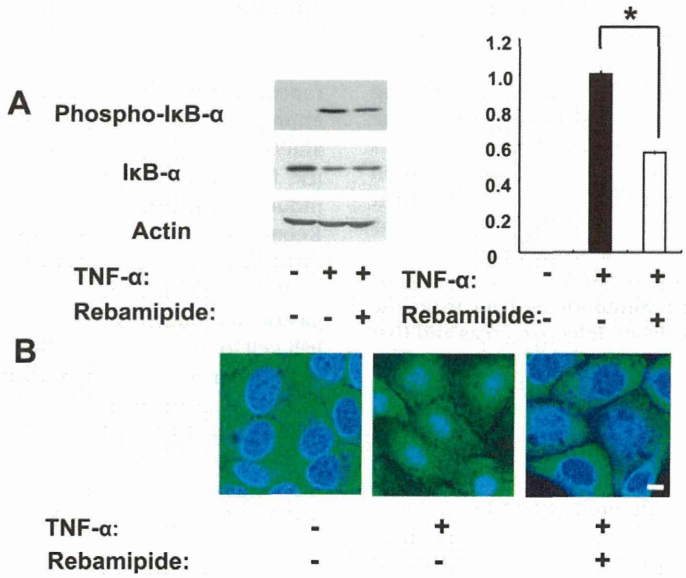

FIGURE 4. Inhibition by rebamipide of the TNF-α–induced activation of the NF-κB signaling pathway in HCE cells. (**A**) Cells were incubated for 12 hours in the absence or presence of rebamipide (0.3 mM) and then for 30 minutes in the additional absence or presence of TNF-α. Cell lysates were then prepared and subjected to immunoblot analysis with antibodies to IκB-α or to phosphorylated IκB-α (*left panel*). The amount of phosphorylated IκB-α was determined by densitometric scanning of immunoblots and normalized by the corresponding amount of β-actin (*right panel*); data are expressed relative to the normalized value for cells treated with TNF-α alone and are means ± SEM from three independent experiments. *$P < 0.05$ (ANOVA followed by Dunnett's test). (**B**) Cells were incubated for 12 hours in the absence or presence of rebamipide (0.3 mM) and then for 30 minutes in the additional absence or presence of TNF-α. They were then fixed, permeabilized, and subjected to immunofluorescence analysis with antibodies to the p65 subunit of NF-κB (*green signal*). Nuclei were detected by staining with Cyto59 (*blue signal*). *Scale bar*: 10 μm.

Investigative Ophthalmology & Visual Science

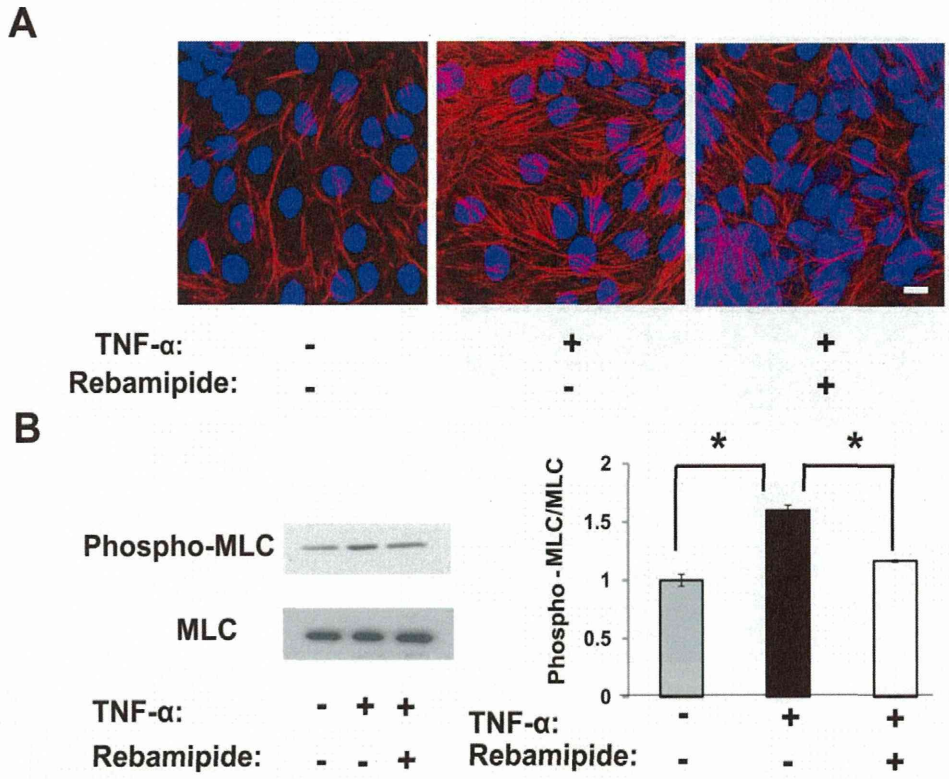

FIGURE 5. Inhibition by rebamipide of the TNF-α–induced reorganization of the actin cytoskeleton and MLC phosphorylation in HCE cells. (**A**) Cells were incubated in the absence or presence of rebamipide (0.3 mM) for 12 hours and then in the additional absence or presence of TNF-α for 24 hours. They were then fixed and stained with rhodamine-phalloidin to detect actin filaments (*red signal*) and with Cyto59 to detect nuclei (*blue signal*). *Scale bar*: 10 μm. (**B**) Cells were incubated in the absence or presence of rebamipide (0.3 mM) for 12 hours and then in the additional absence or presence of TNF-α for 24 hours. Cell lysates were then prepared and subjected to immunoblot analysis with antibodies to phosphorylated MLC and to MLC (*left panel*). The amount of phosphorylated MLC was determined by densitometric scanning of immunoblots and normalized by the corresponding amount of MLC (*right panel*); data are expressed relative to the normalized value for cells incubated without addition and are means ± SEM from three independent experiments. $^*P < 0.05$ (ANOVA followed by Dunnett's test).

actin cytoskeleton in these cells, and that such modulation may contribute to the protection of barrier function.

Rebamipide reduced the concentrations of TNF-α and IL-1β in serum as well as suppressed gastric inflammation in mice infected with *Helicobacter pylori*.[45] It also inhibited the expression of IL-8 induced by TNF-α in human umbilical vein endothelial cells.[46] Corneal epithelial disorders are associated with various ocular surface diseases involving inflammation.[47] We have now shown that rebamipide attenuated TNF-α–induced barrier disruption in HCE cells as well as ameliorated corneal epithelial damage in a rat model of dry eye. The levels of IL-1β and TNF-α at the ocular surface were previously found

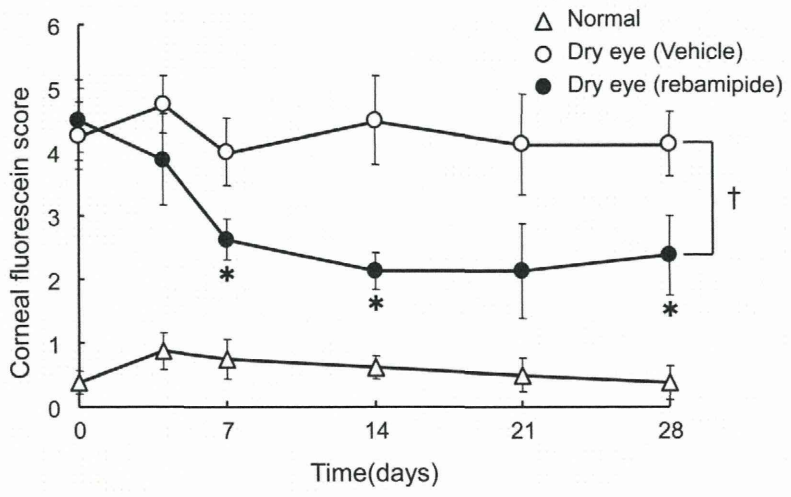

FIGURE 6. Effect of rebamipide eyedrops on corneal epithelial damage in a rat model of dry eye. Corneal epithelial damage induced by removal of lacrimal glands was evaluated by fluorescein staining at the indicated times after the onset of treatment four times daily with eyedrops containing 2% rebamipide or vehicle. The cornea of nontreated healthy rats was evaluated as a normal control. Data are means ± SEM for both eyes of eight rats per group. $^*P < 0.05$ versus the corresponding value for vehicle treatment (Student's unpaired *t*-test). $\dagger P < 0.05$ (ANOVA for repeated measures).

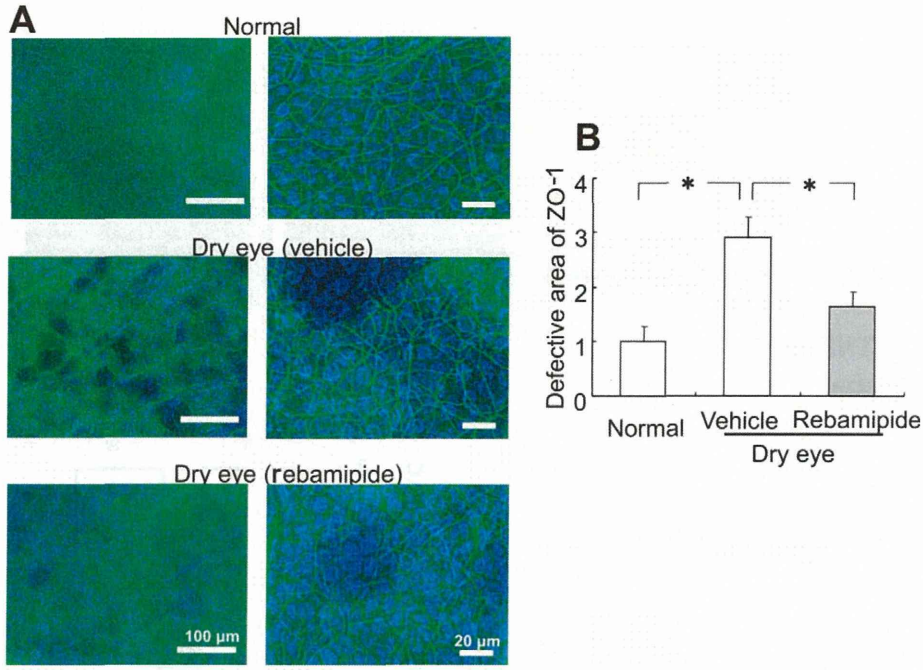

FIGURE 7. Effect of rebamipide eyedrops on the distribution of ZO-1 in the corneal epithelium of a rat model of dry eye. (**A**) Corneal tissue blocks prepared from a healthy eye or from eyes of a dry eye model treated with vehicle or rebamipide for 28 days were subjected to immunofluorescence staining with antibodies to ZO-1 (*green signal*) and to staining of nuclei with 4′,6-diamidino-2-phenylindole (*blue signal*). *Scale bars*: 100 μm (*left panels*), 20 μm (*right panels*). (**B**) The area of the corneal epithelium in which cells show loss of ZO-1 immunoreactivity from cell–cell borders was determined by image analysis and expressed relative to the value for healthy eyes. Data are means ± SEM for both eyes of four rats per group. $^*P < 0.05$ (unpaired Student's *t*-test).

to be increased in a dry eye model.[26] These various observations suggest that rebamipide may suppress ocular inflammation, and thereby help to maintain the integrity of the corneal epithelium. Indeed, rebamipide has recently been applied clinically to the treatment of patients with dry eye symptoms in Japan. Further investigations are warranted to determine the clinical efficacy of rebamipide for other ocular inflammatory disorders.

TNF-α induces the expression of matrix metalloproteinases (MMPs) in certain cell types.[48,49] Activation of MMP-9 at the ocular surface in experimental dry eye has been shown to promote disruption of corneal epithelial barrier function as a result of the loss of TJs from superficial corneal epithelial cells.[50] Signaling by NF-κB contributes to the expression of MMPs.[51,52] Rebamipide reduced the expression of MMP-13 in human chondrocytes.[53] We have now shown that rebamipide inhibited the TNF-α–induced activation of NF-κB and downregulation of ZO-1 in HCE cells. These results suggest that rebamipide may suppress TNF-α–induced expression of MMPs through inhibition of NF-κB activation, thereby, attenuating the proteolysis of ZO-1 in HCE cells. TNF-α also promotes the release of intracellular free radicals,[54] which have been found to contribute to disruption of endothelial barrier function,[55] and rebamipide is thought to act as a radical scavenger.[32]

Ocular inflammation can lead to increased corneal epithelial permeability as a result of disruption of TJ structure. TNF-α plays an important role in corneal epithelial diseases associated with ocular inflammation. Inhibition of the adverse effects of TNF-α on corneal epithelial barrier function by rebamipide is, thus, a potential new approach to the treatment of corneal epithelial disorders associated with ocular inflammation.

Acknowledgments

The authors thank Yukari Mizuno, Shizuka Murata, and Eriko Yamanaga as well as the staff of the Institute of Laboratory Animals at Yamaguchi University for their technical assistance.

Supported by MEXT/JSPS KAKENHI Grant 23592572 from Ministry of Education, Culture, Sports, Science and Technology-Japan.

Disclosure: **K. Kimura**, None; **Y. Morita**, None; **T. Orita**, None; **J. Haruta**, None; **Y. Takeji**, None; **K.-H. Sonoda**, None

References

1. Prausnitz MR, Noonan JS. Permeability of cornea, sclera, and conjunctiva: a literature analysis for drug delivery to the eye. *J Pharm Sci*. 1998;87:1479–1488.
2. Kinoshita S, Adachi W, Sotozono C, et al. Characteristics of the human ocular surface epithelium. *Prog Retin Eye Res*. 2001; 20:639–673.
3. Kalinin AE, Kajava AV, Steinert PM. Epithelial barrier function: assembly and structural features of the cornified cell envelope. *Bioessays*. 2002;24:789–800.
4. Ebnet K, Suzuki A, Ohno S, Vestweber D. Junctional adhesion molecules (JAMs): more molecules with dual functions? *J Cell Sci*. 2004;117:19–29.
5. Harhaj NS, Antonetti DA. Regulation of tight junctions and loss of barrier function in pathophysiology. *Int J Biochem Cell Biol*. 2004;36:1206–1237.
6. Prada J, Noelle B, Baatz H, Hartmann C, Pleyer U. Tumour necrosis factor alpha and interleukin 6 gene expression in keratocytes from patients with rheumatoid corneal ulcerations. *Br J Ophthalmol*. 2003;87:548–550.
7. Collares-Buzato CB, Jepson MA, Simmons NL, Hirst BH. Increased tyrosine phosphorylation causes redistribution of adherens junction and tight junction proteins and perturbs

paracellular barrier function in MDCK epithelia. *Eur J Cell Biol.* 1998;76:85-92.

8. Stevenson BR, Anderson JM, Bullivant S. The epithelial tight junction: structure, function and preliminary biochemical characterization. *Mol Cell Biochem.* 1988;83:129-145.
9. Anderson JM, Fanning AS, Lapierre L, Van Itallie CM. Zonula occludens (ZO)-1 and ZO-2: membrane-associated guanylate kinase homologues (MAGuKs) of the tight junction. *Biochem Soc Trans.* 1995;23:470-475.
10. Aberle H, Schwartz H, Kemler R. Cadherin-catenin complex: protein interactions and their implications for cadherin function. *J Cell Biochem.* 1996;61:514-523.
11. Giehl K, Menke A. Microenvironmental regulation of E-cadherin-mediated adherens junctions. *Front Biosci.* 2008; 13:3975-3985.
12. Schnittler HJ. Structural and functional aspects of intercellular junctions in vascular endothelium. *Basic Res Cardiol.* 1998; 93;30-39.
13. Miyoshi J, Takai Y. Molecular perspective on tight-junction assembly and epithelial polarity. *Adv Drug Deliv Rev.* 2005;57: 815-855.
14. Ban Y, Dota A, Cooper LJ, et al. Tight junction-related protein expression and distribution in human corneal epithelium. *Exp Eye Res.* 2003;76:663-669.
15. Scott RA, Lauweryns B, Snead DM, Haynes RJ, Mahida Y, Dua HS. E-cadherin distribution and epithelial basement membrane characteristics of the normal human conjunctiva and cornea. *Eye (Lond).* 1997;11;607-612.
16. Yoshida Y, Ban Y, Kinoshita S. Tight junction transmembrane protein claudin subtype expression and distribution in human corneal and conjunctival epithelium. *Invest Ophthalmol Vis Sci.* 2009;50:2103-2108.
17. Yi X, Wang Y, Yu FS. Corneal epithelial tight junctions and their response to lipopolysaccharide challenge. *Invest Ophthalmol Vis Sci.* 2000;41:4093-4100.
18. Langbein L, Grund C, Kuhn C, et al. Tight junctions and compositionally related junctional structures in mammalian stratified epithelia and cell cultures derived therefrom. *Eur J Cell Biol.* 2002;81:419-435.
19. Moore P, Ogilvie J, Horridge E, Mellor IR, Clothier RH. The development of an innervated epithelial barrier model using a human corneal cell line and ND7/23 sensory neurons. *Eur J Cell Biol.* 2005;84:581-592.
20. Sugrue SP, Zieske JD. ZO1 in corneal epithelium: association to the zonula occludens and adherens junctions. *Exp Eye Res.* 1997;64:11-20.
21. Kimura K, Teranishi S, Fukuda K, Kawamoto K, Nishida T. Delayed disruption of barrier function in cultured human corneal epithelial cells induced by tumor necrosis factor-alpha in a manner dependent on NF-kappaB. *Invest Ophthalmol Vis Sci.* 2008;49:565-571.
22. Kimura K, Teranishi S, Nishida T. Interleukin-1beta-induced disruption of barrier function in cultured human corneal epithelial cells. *Invest Ophthalmol Vis Sci.* 2009;50:597-603.
23. Cordingley FT, Bianchi A, Hoffbrand AV, et al. Tumour necrosis factor as an autocrine tumour growth factor for chronic B-cell malignancies. *Lancet.* 1988;1:969-971.
24. Keadle TL, Usui N, Laycock KA, Miller JK, Pepose JS, Stuart PM. IL-1 and TNF-alpha are important factors in the pathogenesis of murine recurrent herpetic stromal keratitis. *Invest Ophthalmol Vis Sci.* 2000;41:96-102.
25. Planck SR, Rich LF, Ansel JC, Huang XN, Rosenbaum JT. Trauma and alkali burns induce distinct patterns of cytokine gene expression in the rat cornea. *Ocul Immunol Inflamm.* 1997;5:95-100.
26. Luo L, Li DQ, Doshi A, Farley W, Corrales RM, Pflugfelder SC. Experimental dry eye stimulates production of inflammatory cytokines and MMP-9 and activates MAPK signaling pathways on the ocular surface. *Invest Ophthalmol Vis Sci.* 2004;45: 4293-4301.
27. Cameron JA. Shield ulcers and plaques of the cornea in vernal keratoconjunctivitis. *Ophthalmology.* 1995;102:985-993.
28. Stern ME, Pflugfelder SC. Inflammation in dry eye. *Ocul Surf.* 2004;2:124-130.
29. Lam H, Bleiden L, de Paiva CS, Farley W, Stern ME, Pflugfelder SC. Tear cytokine profiles in dysfunctional tear syndrome. *Am J Ophthalmol.* 2009;147:198-205. e191.
30. De Paiva CS, Corrales RM, Villarreal AL, et al. Corticosteroid and doxycycline suppress MMP-9 and inflammatory cytokine expression, MAPK activation in the corneal epithelium in experimental dry eye. *Exp Eye Res.* 2006;83:526-535.
31. Zhu L, Shen J, Zhang C, et al. Inflammatory cytokine expression on the ocular surface in the Botulium toxin B induced murine dry eye model. *Mol Vis.* 2009;15:250-258.
32. Arakawa T, Kobayashi K, Yoshikawa T, Tarnawski A. Rebamipide: overview of its mechanisms of action and efficacy in mucosal protection and ulcer healing. *Dig Dis Sci.* 1998;43: 5S-13S.
33. Katada K, Yoshida N, Isozaki Y, et al. Prevention by rebamipide of acute reflux esophagitis in rats. *Dig Dis Sci.* 2005;50:S97-S103.
34. Qi Z, Jie L, Haixia C, Xiaoying Z. Effect of rebamipide on quality of peptic ulcer healing in rat. *Dig Dis Sci.* 2009;54: 1876-1883.
35. Tanito M, Takanashi T, Kaidzu S, Yoshida Y, Ohira A. Cytoprotective effects of rebamipide and carteolol hydrochloride against ultraviolet B-induced corneal damage in mice. *Invest Ophthalmol Vis Sci.* 2003;44:2980-2985.
36. Araki-Sasaki K, Ohashi Y, Sasabe T, et al. An SV40-immortalized human corneal epithelial cell line and its characterization. *Invest Ophthalmol Vis Sci.* 1995;36:614-621.
37. Fujihara T, Murakami T, Fujita H, Nakamura M, Nakata K. Improvement of corneal barrier function by the P2Y(2) agonist INS365 in a rat dry eye model. *Invest Ophthalmol Vis Sci.* 2001;42:96-100.
38. Joh T, Takezono Y, Oshima T, et al. The protective effect of rebamipide on paracellular permeability of rat gastric epithelial cells. *Aliment Pharmacol Ther.* 2003;18:133-138.
39. Matysiak-Budnik T, Thomas-Collignon A, Megraud F, Heyman M. Alterations of epithelial permeability by Helicobacter and IL-1beta in vitro: protective effect of rebamipide. *Dig Dis Sci.* 2001;46:1558-1566.
40. Turner JR. 'Putting the squeeze' on the tight junction: understanding cytoskeletal regulation. *Semin Cell Dev Biol.* 2000;11:301-308.
41. Wittchen ES, Haskins J, Stevenson BR. Protein interactions at the tight junction. Actin has multiple binding partners, and ZO-1 forms independent complexes with ZO-2 and ZO-3. *J Biol Chem.* 1999;274:35179-35185.
42. Shen L, Turner JR. Actin depolymerization disrupts tight junctions via caveolae-mediated endocytosis. *Mol Biol Cell.* 2005;16:3919-3936.
43. Torii H, Kubota H, Ishihara H, Suzuki M. Cilostazol inhibits the redistribution of the actin cytoskeleton and junctional proteins on the blood-brain barrier under hypoxia/reoxygenation. *Pharmacol Res.* 2007;55:104-110.
44. Wang F, Graham WV, Wang Y, Witkowski ED, Schwarz BT, Turner JR. Interferon-gamma and tumor necrosis factor-alpha synergize to induce intestinal epithelial barrier dysfunction by up-regulating myosin light chain kinase expression. *Am J Pathol.* 2005;166:409-419.
45. Hahm KB, Kim DH, Lee KM, et al. Effect of long-term administration of rebamipide on *Helicobacter pylori* infection in mice. *Aliment Pharmacol Ther.* 2003;18:24-38.

46. Choe JY, Park KY, Lee SJ, Park SH, Kim SK. Rebamipide inhibits tumor necrosis factor-alpha-induced interleukin-8 expression by suppressing the NF-kappaB signal pathway in human umbilical vein endothelial cells. *Inflamm Res.* 59:1019–1026.
47. De Nicola R, Labbe A, Amar N, Dupas B, Baudouin C. In vivo confocal microscopy and ocular surface diseases: anatomical-clinical correlations [in French]. *J Fr Ophtalmol.* 2005;28:691–698.
48. Ikebe T, Takeuchi H, Jimi E, Beppu M, Shinohara M, Shirasuna K. Involvement of proteasomes in migration and matrix metalloproteinase-9 production of oral squamous cell carcinoma. *Int J Cancer.* 1998;77:578–585.
49. Janowska-Wieczorek A, Marquez LA, Nabholtz JM, et al. Growth factors and cytokines upregulate gelatinase expression in bone marrow CD34(+) cells and their transmigration through reconstituted basement membrane. *Blood.* 1999;93: 3379–3390.
50. Pflugfelder SC, Farley W, Luo L, et al. Matrix metalloproteinase-9 knockout confers resistance to corneal epithelial barrier disruption in experimental dry eye. *Am J Pathol.* 2005;166: 61–71.
51. Andela VB, Gordon AH, Zotalis G, et al. NFkappaB: a pivotal transcription factor in prostate cancer metastasis to bone. *Clin Orthop Relat Res.* 2003;S75–85.
52. Das R, Philip S, Mahabeleshwar GH, Bulbule A, Kundu GC. Osteopontin: its role in regulation of cell motility and nuclear factor kappa B-mediated urokinase type plasminogen activator expression. *IUBMB Life.* 2005;57:441–447.
53. Moon SJ, Woo YJ, Jeong JH, et al. Rebamipide attenuates pain severity and cartilage degeneration in a rat model of osteoarthritis by downregulating oxidative damage and catabolic activity in chondrocytes. *Osteoarthritis Cartilage.* 2012;20:1426–1438.
54. Tsuji S, Kawai N, Tsujii M, Kawano S, Hori M. Review article: inflammation-related promotion of gastrointestinal carcinogenesis–a perigenetic pathway. *Aliment Pharmacol Ther.* 2003;18:82–89.
55. Fraser PA. The role of free radical generation in increasing cerebrovascular permeability. *Free Radic Biol Med.* 2011:51: 967–977.

Investigative Ophthalmology & Visual Science

THE JOURNAL OF IMMUNOLOGY

IL-23–Independent Induction of IL-17 from γδT Cells and Innate Lymphoid Cells Promotes Experimental Intraocular Neovascularization

Eiichi Hasegawa, Koh-Hei Sonoda, Takashi Shichita, Rimpei Morita, Takashi Sekiya, Akihiro Kimura, Yuji Oshima, Atsunobu Takeda, Takeru Yoshimura, Shigeo Yoshida, Tatsuro Ishibashi and Akihiko Yoshimura

J Immunol 2013; 190:1778-1787; Prepublished online 14 January 2013;
doi: 10.4049/jimmunol.1202495
http://www.jimmunol.org/content/190/4/1778

The Journal of Immunology is published twice each month by
The American Association of Immunologists, Inc.,
9650 Rockville Pike, Bethesda, MD 20814-3994.

Print ISSN: 0022-1767 Online ISSN: 1550-6606.

IL-23–Independent Induction of IL-17 from γδT Cells and Innate Lymphoid Cells Promotes Experimental Intraocular Neovascularization

Eiichi Hasegawa,*,†,‡ Koh-Hei Sonoda,§ Takashi Shichita,*,† Rimpei Morita,*,† Takashi Sekiya,*,† Akihiro Kimura,*,† Yuji Oshima,‡ Atsunobu Takeda,‡ Takeru Yoshimura,‡ Shigeo Yoshida,‡ Tatsuro Ishibashi,‡ and Akihiko Yoshimura*,†

Choroidal neovascularization (CNV) is a characteristic of age-related macular degeneration. Genome-wide association studies have provided evidence that the immune system is involved in the pathogenesis of age-related macular degeneration; however, the role of inflammatory cytokines in CNV has not been established. In this study, we demonstrated that IL-17 had a strong potential for promoting neovascularization in a vascular endothelial growth factor–independent manner in laser-induced experimental CNV in mice. Infiltrated γδT cells and Thy-1$^+$ innate lymphoid cells, but not Th17 cells, were the main sources of IL-17 in injured eyes. IL-23 was dispensable for IL-17 induction in the eye. Instead, we found that IL-1β and high-mobility group box 1 strongly promoted IL-17 expression by γδT cells. Suppression of IL-1β and high-mobility group box 1, as well as depletion of γδT cells, reduced IL-17 levels and ameliorated experimental CNV. Our findings suggest the existence of a novel inflammatory cytokine network that promotes neovascularization in the eye. *The Journal of Immunology*, **2013, 190: 1778–1787.**

Age-related macular degeneration (AMD) is the leading cause of irreversible visual impairment in persons aged 60 y and older in Western countries (1). The pathogenesis of AMD is complex and not well established. Chronic local inflammation from persistent infection was recently identified as a candidate etiology for AMD. Choroidal neovascularization (CNV), the hallmark of wet AMD, was shown to be dependent on inflammatory cytokines, as well as inflammatory signals. Genetic studies also demonstrated strong associations between AMD and several gene variants in genes coding for inflammatory mediators and complement proteins (1–3).

CNV consists of new blood vessel growth from the choroid extending into the subretinal space. These immature vessels easily permit subretinal bleeding or extravascular leakage of blood components, causing injury to the retina. Vascular endothelial growth factor (VEGF) from retinal pigment epithelium (RPE) cells and infiltrating macrophages has been considered the most important factor for CNV development (4, 5). NKT cells, as well as inflammatory cytokines, such as IL-1β, IL-6, and TGF-β, were shown to promote CNV, whereas IL-27 suppresses it by modulating VEGF levels (6–9).

IL-17 is a major proinflammatory cytokine linked to the pathogenesis of diverse autoimmune and inflammatory diseases, such as rheumatoid arthritis (RA), psoriasis, inflammatory bowel disease, and uveitic diseases. Of note, IL-17 was shown to be proangiogenic and to induce endothelial cell invasion (10). IL-17 has the potential to upregulate VEGF from RA synoviocytes (11) and to promote the development of microvessel structures in RA, as well as in tumor growth (12, 13). Recently, a subset of effector Th cells, the IL-17–producing T cell (Th17), was implicated in the pathogenesis of various autoimmune diseases, including uveitis, arthritis, multiple sclerosis, psoriasis, and inflammatory bowel disease. In addition, γδT cells, as well as innate lymphoid cells (ILCs), have been implicated as IL-17–producing cells (14). A recent study suggested that C5a promoted IL-22 and IL-17 expression from CD4$^+$ T cells in AMD patients (15). Intriguingly, this study found significantly increased levels of IL-22 and IL-17 in the sera of AMD patients, suggesting possible roles for IL-22 and IL-17 in the inflammation that contributes to CNV and AMD. However, the role of IL-17 and mechanism of IL-17 expression in experimental CNV have not been investigated.

In this study, using gene-disrupted mice and inoculation with Abs, we demonstrated that IL-17 is essential for the development of laser-induced CNV. We identified infiltrated γδT cells, but not Th17 cells, along with Thy-1$^+$ ILCs as the main sources of IL-17 in the laser-treated eye. Furthermore, we found that IL-1β and high-mobility group box 1 (HMGB-1), rather than IL-23, play critical roles in the infiltration of IL-17–producing cells. Moreover, IL-1β, HMGB-1, and γδT cells were shown to be essential for inducing IL-17, and suppression of these cytokines/cells was therapeutic for

*Department of Microbiology and Immunology, Keio University School of Medicine, Shinjuku-ku, Tokyo 160-8582, Japan; †Japan Science and Technology Agency, Core Research for Evolutional Science and Technology, Chiyoda-ku, Tokyo 102-0075, Japan; ‡Department of Ophthalmology, Graduate School of Medical Sciences, Kyushu University, Fukuoka 812-8582, Japan; and §Department of Ophthalmology, Yamaguchi University Graduate School of Medicine, Ube, Yamaguchi 755-8505, Japan

Received for publication September 5, 2012. Accepted for publication December 9, 2012.

This work was supported by special grants-in-aid from the Ministry of Education, Culture, Sports, Science and Technology of Japan; the Program for the Promotion of Fundamental Studies in Health Science of the National Institute of Biomedical Innovation; the SENSIN Medical Research Foundation; the Mochida Memorial Foundation; the Uehara Memorial Foundation; and the Takeda Science Foundation.

Address correspondence and reprint requests to Prof. Akihiko Yoshimura, Department of Microbiology and Immunology, Keio University School of Medicine, 35 Shinanomachi, Shinjuku-ku, Tokyo 160-8582, Japan. E-mail address: yoshimura@a6.keio.jp

Abbreviations used in this article: AMD, age-related macular degeneration; CNV, choroidal neovascularization; DAMP, damage-associated molecular pattern molecule; HMGB-1, high-mobility group box 1; ILC, innate lymphoid cell; iNKT, invariant NKT; KO, knockout; PC, laser photocoagulation; RA, rheumatoid arthritis; RPE, retinal pigment epithelium; VEGF, vascular endothelial growth factor; WT, wild-type.

www.jimmunol.org/cgi/doi/10.4049/jimmunol.1202495

experimental CNV. Our study indicates that IL-17 plays a central role in CNV and could serve as a therapeutic target for AMD.

Materials and Methods

Animals

C57BL/6 (wild-type [WT]) mice, 6–10 wk of age, were purchased from CLEA (Tokyo, Japan) and were kept under specific pathogen–free conditions at Keio University. IL-17 knockout (KO) (16) and IL-23p19 KO (17) mice were described previously. RAG2 KO and TCRγδ KO mice were purchased from The Jackson Laboratory (Bar Harbor, ME). TLR2 and TLR4 KO mice were provided by Dr. S. Akira (Laboratory of Host Defense, Osaka University, Osaka, Japan). All mice were on the C57BL/6 background. All animal experiments were conducted in accordance with the Association for Research in Vision and Ophthalmology Statement for the Use of Animals.

Induction and evaluation of CNV

CNV was induced by laser photocoagulation (PC) and evaluated as described previously (18). Briefly, PC (wavelength = 532 nm, 0.1 s, spot size = 75 μm, power = 200 mW) was performed at four spots around the optic disc of one eye of each mouse. Abs and recombinant proteins were inoculated into the vitreous cavities with a microsyringe immediately after laser treatment. On day 7 after laser treatment, the mice were perfused with 1 ml PBS containing 50 mg/ml fluorescent-labeled dextran (25,000 m.w.; Sigma-Aldrich, St. Louis, MO), and the eyes were removed. The entire retina was carefully dissected from the eyecup and flat-mounted on an aqua-mount with the sclera facing downward and the choroid facing upward. The images were captured using conventional fluorescence microscopy (BZ-8000; Keyence) for CNV area measurement or confocal laser microscopy (LSM510 META; Carl Zeiss) for CNV volume measurement. The hyperfluorescent area and volume corresponding to a photocoagulation spot for each treated eye was evaluated using ImageJ software and subjected to semiquantitative analysis.

Vitreous cavity injection

rIL-17, anti–IL-17 Ab, anti-VEGFA Ab, and rIL-1ra (R&D Systems, Minneapolis, MN) were inoculated into the vitreous cavity using fine, 32-Ga needles (cat. no. 0160832) and 10-μl syringes (cat. no. 80330; both from Hamilton, Reno, NV). The tip of the needle penetrated the sclera, choroid, and retina to reach the vitreous cavity, and a maximum volume of 2 μl/injection was applied per eye. We ensured that the Ag was injected into the vitreous cavity by carefully guiding the tip of the needle under the microscope, through the flattened cornea, which was covered by a glass microscope slide. Inoculating 2 μl solution increased the intraocular pressure sufficiently to seal the retinal incision completely without bleeding or detachment. We considered the total volume of the murine eye to be 10 μl; therefore, 2 μl inoculated Ab solution was diluted five times in vivo. The concentration of each inoculating Ab/recombinant cytokine was determined according to the manufacturer's instructions so as to be sufficient for neutralization or supplementation in vivo.

Real-time RT-PCR

Total RNA was extracted from whole eyes, with the exception of the conjunctiva. Samples from two eyes were pooled to obtain a sufficient amount of mRNA for analysis. The RNA was extracted using Sepasol-RNA I Super G (Nacalai Tesque, Kyoto, Japan), according to the manufacturer's instructions. RNA was reverse transcribed to cDNA with random primers and a high-capacity cDNA reverse transcription kit (both from Applied Biosystems, Carlsbad, CA), in accordance with the manufacturer's instructions. Gene expression was examined using a Bio-Rad (Hercules, CA) iCycler Optical System and SsoFast EvaGreen Supermix. The results were normalized to *HPRT* levels. The primers used were as follows: 5′-CAGCAGCGATCATCCCTCAAAG-3′ and 5′-CAGGACCAGGATCTCTTGCTG-3′ for *IL-17*; 5′-CAGGCAGGCAGTATCACTCA-3′ and 5′-AGGCCACAGGTATTTTGTCG-3′ for *IL-1β*; 5′-ACCTCCACTGCCAGCTGTGTGCTG-TC-3′ and 5′-TCATTTCTGCACTTCTGCATGTAGACTGTCCC-3′ for *RORγt*; 5′-TGAAGAGCTACTGTAATGATCAGTCAAC-3′ and 5′-AGCAAGCTTGCAACCTTAACCA-3′ for *HPRT*; and 5′-CCATTGGTGATGTTGCAAAG-3′ and 5′-CTTTTTCGCTGCATCAGGTT-3′ for *HMGB-1*.

Immunohistochemistry

As reported previously (19), hamster anti-mouse TCRγδ (BD Biosciences, Franklin Lakes, NJ) and rabbit polyclonal anti–HMGB-1 (Abcam, Cambridge, U.K.) were used as primary Abs and incubated at 4°C overnight. Goat anti-rabbit IgG conjugated to Alexa Fluor 488 was used as a secondary Ab and incubated at room temperature for 1 h.

Isolation of ocular-infiltrating cells and flow cytometric analysis

To examine phenotypes, ocular-infiltrating cells were prepared as described previously (5). After PC, the eyes were enucleated, and the posterior segments of two eyes were used for FACS analysis. For intracellular cytokine staining, cells were stimulated for 4.5 h in complete medium with phorbol 12-myristate 13-acetate (50 ng/ml) and ionomycin (500 ng/ml; both from Sigma-Aldrich) in the presence of brefeldin A (eBioscience, San Diego, CA). Surface staining was then performed in the presence of Fc-blocking Abs (2.4G2), followed by intracellular staining for cytokines with a fixation and permeabilization kit (eBioscience), according to the manufacturer's instructions. All Abs were obtained from eBioscience. Data were acquired using a BD FACSAria or BD FACSCanto II and were analyzed with FlowJo software (Tree Star, Ashland, OR).

Transfer of γδT cells or CD4$^+$ T cells into Rag2 *KO mice*

CD3$^+$ T lymphocytes were prepared from the spleens and lymph nodes of WT mice by negative selection using magnetic beads (Miltenyi Biotec, Bergisch Gladbach, Germany) (typically >95% purity) (20). A total of 3×10^5 CD3$^+$CD4$^-$TCRγδ$^+$ cells from WT mice or 1×10^6 CD3$^+$CD4$^+$ TCRγδ$^-$ cells from WT mice, purified through flow cytometry, was injected i.v. into *Rag2* KO mice. Four days after cell transfer, the mice were subjected to laser treatment; 1 wk later, the eyes were enucleated for evaluation of CNV.

In vitro assay

A total of 1×10^5 CD3$^+$CD4$^-$TCRγδ$^+$ T cells was cultured for 48 h with 1 ng/ml plate-bound anti-CD3 Ab (clone 145-2C11) in the presence of 0.1–10 ng/ml rIL-1β (PeproTech, London, U.K.), 1 ng/ml IL-23 (PeproTech), or 1 μg/ml HMGB-1 (Shino-Test, Tokyo, Japan). The amount of secreted IL-17 protein in the supernatants was measured using ELISA (eBioscience), according to the manufacturer's instructions.

Statistical analyses

All data are expressed as mean ± SE and were analyzed using the Dunnett test and the independent-samples t test. The p values < 0.05 were considered statistically significant.

Results

IL-17 promotes choroidal neovascularization after laser treatment

Because a recent report (15) showed a significant increase in IL-17 levels in the sera of AMD patients, we investigated the role of IL-17 in laser-induced CNV in mice. After laser treatment to the eye, expression of *Il17a* mRNA significantly increased from day 3, peaked at day 4, and then gradually decreased (Fig. 1A). To investigate the functional role of IL-17 in ocular neovascularization, *Il17a*-deficient (IL-17 KO) mice were examined. On day 7 after laser treatment, CNV was visualized by the perfusion of fluorescent-labeled dextran, and the green neovascularized areas were measured on choroidal flat mounts. Compared with control mice, IL-17 KO mice exhibited significantly smaller areas of CNV (Fig. 1B). In contrast, areas of CNV were significantly larger in WT mice inoculated with rIL-17 than in untreated WT mice (Fig. 1C). These data indicate that IL-17 promotes CNV development.

We investigated the relationship between IL-17 and VEGF. Unexpectedly, WT and IL-17 KO mice had similar VEGF mRNA levels in their injured eyes (Fig. 1D). Next, we compared the effect of depletion of VEGF and IL-17 on CNV development using Abs. When anti–IL-17 Ab was inoculated into the vitreous cavity, CNV volume was reduced (Fig. 1E, 1F). The suppressive effect of anti–IL-17 Ab on CNV volume and area was similar to that of anti-VEGF